

April 15, 1998

PROPOSAL

Ionization Cooling Research and Development Program for a High Luminosity Muon Collider

Charles M. Ankenbrandt^a, Muzaffer Atac^a, Giorgio Apollinari^b, Valeri I. Balbekov^a, Morris Binkley^a, S. Alex Bogacz^c, Christine Celata^d, David B. Cline^e, John Corlett^d, Lucien M. Cremaldi^f, Richard C. Fernow^g, David Finley^a, Yasuo Fukui^h, Juan C. Gallardo^g, Stephen H. Geer^{a,†}, Gail G. Hanson^o, Ahmed Hassaneinⁱ, Carol Johnstone^a, Stephen A. Kahn^g, Bruce J. King^g, Harold G. Kirk^g, Thomas R. Kobilarcik^a, Yoshitaka Kuno^h, Paul LeBrun^a, Kevin Lee^e, Derun Li^d, Changguo Lu^j, Kirk T. McDonald^j, Alfred D. McInturff^d, Frederick E. Mills^a, Nikolai V. Mokhov^a, Alfred Moretti^a, Yoshiharu Mori^h, David V. Neuffer^a, Robert J. Noble^a, James H. Norem^{a,i}, Stephen C. O'Day^a, Yasar Onel^k, Robert B. Palmer^g, Zohreh Parsa^g, Yuriy Pischalnikov^e, Milorad Popovic^a, Eric J. Prebys^j, Zubao Qian^a, Rajendran Raja^a, Claude Reedⁱ, Pavel Rehak^g, Andrew M. Sessler^d, Gregory I. Silvestrov^l, Alexandr N. Skrinsky^l, Dale Smithⁱ, Panagiotis G. Spentzouris^a, Ray Stefanski^a, Sergei Striganov^a, Donald J. Summers^f, Lee C. Tengⁱ, Alvin V. Tollestrup^a, William C. Turner^d, Andreas Van Ginneken^a, Tatiana A. Vsevolozhskaya^l, David R. Winn^m, Jonathan S. Wurteleⁿ, Takeichiro Yokoi^h, Yongxiang Zhao^g, Max Zolotarev^d

The MUCOOL Collaboration

† Spokesperson

- ^aFermi National Laboratory, P. O. Box 500, Batavia, IL 60510
- ^bRockefeller University, NY
- ^cJefferson Laboratory, 12000 Jefferson Ave., Newport News, VA 23606
- ^dLawrence Berkeley National Laboratory, 1 Cyclotron Rd., Berkeley, CA 94720
- ^eUniversity of California Los Angeles, P. O. Box 951547, Los Angeles, CA 900095
- ^fUniversity of Mississippi, Oxford, MS 38677
- ^gBrookhaven National Laboratory, Upton, NY 11973
- ^hKEK High Energy Research Organization, Tsukuba, Ibaraki, 305-0801, Japan
- ⁱArgonne National Laboratory, Argonne, IL 60439
- ^jJoseph Henry Laboratories, Princeton University, Princeton, NJ 08544
- ^kPhysics Department, Van Allen Hall, University of Iowa, Iowa City, IA 52242
- ^lBudker Institute of Nuclear Physics, 630090 Novosibirsk, Russia
- ^mFairfield University, Fairfield, CT 06430
- ⁿUniversity of California Berkeley, Berkeley, CA 94720
- ^oDepartment of Physics, Indiana University, Bloomington, Indiana 47405

Abstract

We propose a six-year research and development program to develop the hardware needed for ionization cooling, and demonstrate the feasibility of using the ionization cooling technique to produce cooled beams of positive and negative muons for a muon collider. We propose to design and prototype critical sections of the muon ionization cooling channel. These sections would be tested by measuring their performance when exposed to single incoming muons with momenta in the range 100 – 300 MeV/c. The phase-space volume occupied by the population of muons upstream and downstream of the cooling sections would be measured sufficiently well to enable cooling to be demonstrated, the calculations used to design the cooling system to be tested, and optimization of the cooling hardware to be studied.

Contents

1	Executive Summary	5
2	Introduction	8
3	Ionization Cooling	9
3.1	Ionization Cooling Concept	9
3.2	Ionization Cooling Channel	11
4	Cooling Hardware Development	15
4.1	RF Accelerating Structure R&D	16
4.2	Transverse Cooling Channel Development	23
4.3	Wedge Cooling Channel Development	29
4.4	Lithium Lens Research and Development	34
5	Ionization Cooling Test Facility	37
5.1	Low Energy Muon Beamline	38
5.2	Beam Requirements and Muon Rates	40
5.2.1	Fermilab Main Injector Beam Scenario	42
5.2.2	Fermilab Booster Beam Scenario	44
5.3	Measurement Requirements	45
5.4	Detector Design	47
5.4.1	Time Measurement	49
5.4.2	Solenoidal Channel	51
5.4.3	Low-Pressure Time-Projection Chambers	54
5.4.4	Particle Identification	56
5.4.5	Trigger and Data Acquisition	58
5.5	Simulation of the Experiment	59
5.5.1	ICOOL	59
5.5.2	DPGEANT	63
5.6	Cooling Test Facility: Layout and Location	64

6 R & D Plan: Schedule and Funding **67**
6.1 Schedule 67
6.2 Required Facilities at Fermilab 69
6.3 Funding 69

7 Summary **72**

1 Executive Summary

A significant effort is currently being devoted to exploring the feasibility of designing and constructing a high-luminosity muon collider. Of the many technical challenges that have been identified, perhaps the most critical is that of understanding how to produce sufficiently intense beams of positive and negative muons. To accomplish this a new beam cooling technique must be developed. The technique that has been proposed involves passing the beam through an absorber in which the muons lose transverse- and longitudinal-momentum by ionization loss (dE/dx). The longitudinal momentum is then restored by coherent re-acceleration, leaving a net loss of transverse momentum (transverse cooling). The process is repeated many times to achieve a large cooling factor. This cooling technique is called ionization cooling. The beam energy spread can also be reduced using ionization cooling by introducing a transverse variation in the absorber density or thickness (e.g. a wedge) at a location where there is dispersion (the transverse position is energy dependent). Theoretical studies have shown that, assuming realistic parameters for the cooling hardware, ionization cooling can be expected to reduce the phase-space volume occupied by the initial muon beam by a factor of $10^5 - 10^6$.

Ionization cooling is a new technique that has not been demonstrated. Specialized hardware must be developed to perform transverse and longitudinal cooling. It is recognized that understanding the feasibility of constructing an ionization cooling channel that can cool the initial muon beams by factors of $10^5 - 10^6$ is on the critical path to understanding the overall feasibility of the muon collider concept.

We propose to design and prototype critical sections of the muon ionization cooling channel. These sections would be tested by measuring their performance when exposed to single incoming muons with momenta in the range 100 – 300 MeV/c. The phase-space volume occupied by the population of muons upstream and downstream of the cooling sections would be measured sufficiently well to enable cooling to be demonstrated, the calculations used to design the cooling system to be tested, and optimization of the cooling hardware to be studied. Our goal is to develop the muon ionization cooling hardware to the point where a complete ionization cooling channel can be confidently designed for the First Muon Collider.

Initial design studies have shown that a complete cooling channel might consist of 20 – 30 cooling stages, each stage yielding about a factor of two in phase-space reduction.

The early cooling stages focus the beam using a lattice, which consists of solenoids with alternating field directions. Liquid hydrogen absorbers are placed within the solenoids, and RF cavities are placed in matching sections in which the field direction is flipped between the high-field solenoids. To minimize the final transverse emittances that can be achieved, the later cooling sections require the strongest radial focusing that can be achieved in practice. The last few cooling stages therefore use either very high-field (30 T) alternating solenoids, and/or current carrying lithium lenses. The alternating solenoid, wedge, and the lithium lens components will require R&D before a cooling channel can be fully designed. The required alternating solenoid and wedge R&D consists of:

- Developing an appropriate RF re-acceleration structure. To reduce the peak power requirements (by a factor of 2) the RF cells would be operated at liquid nitrogen temperatures, and to maximize the accelerating field on axis the aperture that would be open in a conventional RF cell will be closed by a thin beryllium window. The RF structure must therefore be prototyped and tested at liquid nitrogen temperatures in a solenoidal field before a complete cooling stage can be developed.
- Prototyping a section of an alternating solenoid transverse cooling stage and measuring its performance in a muon beam of the appropriate momentum.
- Prototyping a wedge cooling section and measuring its performance in a muon beam of the appropriate momentum.

The required lithium lens R&D consists of:

- Developing ~ 1 m long liquid lithium lenses. Note that the muon collider repetition rate of 15 Hz would result in a thermal load that would melt a solid lithium rod. Long lenses are required to minimize the number of transitions between lenses.
- Developing lenses with the highest achievable surface fields, and hence the maximum radial focusing, to enable the minimum final emittances to be achieved.
- Prototyping a lens-RF-lens system and measuring its performance in a muon beam of the appropriate momentum.
- Developing, prototyping, and testing a hybrid lithium lens/wedge cooling system.

The measurements that are needed to demonstrate the cooling capability and optimize the design of the alternating solenoid, wedge, and lithium lens cooling stages will require the construction and operation of an ionization cooling test facility. This facility will need (i) a muon beam with a central momentum that can be chosen in the range 100 – 300 MeV/c, (ii) an experimental area that can accommodate a cooling and instrumentation setup of initially ~ 30 m in length, and eventually up to ~ 50 m in length, and (iii) instrumentation to precisely measure the positions of the incoming and outgoing particles in six-dimensional phase-space and confirm that they are muons. In an initial design, the instrumentation consists of identical measuring systems before and after the cooling apparatus. Each measuring system consists of (a) an upstream time measuring device to determine the arrival time of the particles to one quarter of an RF cycle ($\sim \pm 300$ ps), (b) an upstream momentum spectrometer in which the track trajectories are measured by low pressure TPC's on either side of a bent solenoid, (c) an accelerating RF cavity to change the particles momentum by an amount that depends on its arrival time, (d) a downstream momentum spectrometer, which is identical to the upstream spectrometer, and together with the RF cavity and the upstream spectrometer forms a precise time measurement system with a precision of a few ps. The measuring systems are 8 m long, and are contained within a high-field solenoidal channel to keep the beam particles within the acceptance of the cooling apparatus.

The R&D program described in this document can be accomplished in a period of about 6 years. At the end of this period we believe that it will be possible to assess the feasibility and cost of constructing an ionization cooling channel for the First Muon Collider, and begin a detailed design of the complete cooling channel. Our preliminary estimate for the cost of the proposed R&D program is \$37 M. This includes the alternating solenoid, wedge, and lithium lens development, and the instrumentation required for the beam measurements, but does not include the cost of the beamline, experimental hall, or the installation costs, and does not include any contingency.

2 Introduction

A significant effort is currently being devoted to exploring the feasibility of designing and constructing a high-luminosity muon collider [1, 2, 3]. Of the many technical challenges that have been identified, perhaps the most critical is that of understanding how to produce very intense beams of positive and negative muons. This requires maximizing the total number of muons in the colliding beams, while minimizing the phase-space volume they occupy. Unfortunately the muons, which are produced by charged pions decaying within a high-field solenoidal channel, must be collected from a very diffuse phase-space. Indeed, to maximize the total number of muons available for the collider, they must necessarily be collected from as large a phase-space volume as is practical. Hence, before the muons can be accelerated to high energies, the initial phase-space occupied by the muon “beams” must be compressed. To be explicit, to achieve sufficiently intense muon beams for a high luminosity muon collider the phase-space volume must be reduced by about a factor of $10^5 - 10^6$. In particular, a reduction of the normalized horizontal and vertical emittances by two orders of magnitude (from 1×10^{-2} m-rad) is required, together with a reduction of the longitudinal emittance by one to two orders of magnitude.

The technical challenge is to design a system that can reduce the initial muon phase-space by a factor of $10^5 - 10^6$ on a timescale that is short or comparable to the muon lifetime ($\tau_\mu = 2\mu\text{s}$). This time-scale is much shorter than the cooling times that can be achieved using stochastic cooling or electron cooling. Therefore a new cooling technique is needed. The cooling technique that has been proposed for the muon collider is ionization cooling [4, 5, 6, 7, 8, 9, 10, 11]. The feasibility of constructing a muon ionization cooling channel that can achieve the phase-space compression required for a high luminosity muon collider is considered to be one of the most critical items for determining the overall feasibility of the muon collider concept [1].

This proposal describes a six-year research and development program to demonstrate the feasibility of using the ionization cooling technique to produce cool beams of positive and negative muons for a muon collider. We propose to design and prototype critical sections of the muon ionization cooling channel. These sections would be tested by measuring their performance when exposed to single incoming muons with momenta in the range 100 – 300 MeV/c. The phase-space volume occupied by the population of muons upstream and downstream of the cooling sections would be measured sufficiently well to

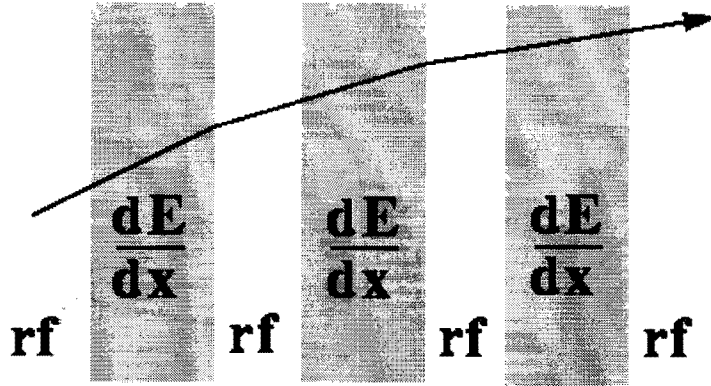


Figure 1: Conceptual schematic of ionization cooling of the transverse phase-space occupied by a muon beam.

enable cooling to be demonstrated, the calculations used to design the cooling system to be tested, and optimization of the cooling hardware to be studied. Our goal is to develop the muon ionization cooling hardware to the point where a complete ionization cooling channel can be confidently designed for the First Muon Collider.

3 Ionization Cooling

Ionization cooling is conceptually simple and is described in Section 3.1. An ionization cooling channel is described in Section 3.2.

3.1 Ionization Cooling Concept

Fig. 1 shows a conceptual schematic of ionization cooling. The beam is passed through some material in which the muons lose both transverse- and longitudinal-momentum by ionization loss (dE/dx). The longitudinal muon momentum is then restored by coherent re-acceleration, leaving a net loss of transverse momentum (transverse cooling). The process is repeated many times to achieve a large cooling factor.

The equation describing transverse cooling (with energies in GeV) is [12, 13]:

$$\frac{d\epsilon_n}{ds} = -\frac{1}{\beta^2} \frac{dE_\mu}{ds} \frac{\epsilon_n}{E_\mu} + \frac{1}{\beta^3} \frac{\beta_\perp (0.014)^2}{2 E_\mu m_\mu L_R}, \quad (1)$$

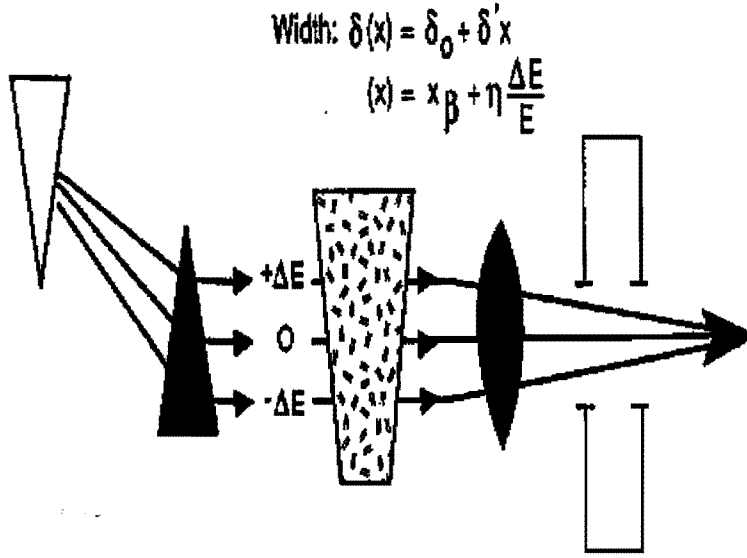


Figure 2: Conceptual schematic of ionization cooling of the longitudinal phase-space using a wedge.

where $\beta = v/c$, ϵ_n is the normalized emittance, β_{\perp} is the betatron function at the absorber, dE_{μ}/ds is the energy loss, and L_R is the radiation length of the material. The first term in this equation is the cooling term, and the second is the heating term due to multiple scattering. This heating term is minimized if β_{\perp} is small (strong-focusing) and L_R is large (a low-Z absorber).

The energy spread is given by:

$$\frac{d(\Delta E)^2}{ds} = -2 \frac{d\left(\frac{dE_{\mu}}{ds}\right)}{dE_{\mu}} \langle (\Delta E_{\mu})^2 \rangle + \frac{d(\Delta E_{\mu})_{\text{straggling}}^2}{ds} \quad (2)$$

where the first term is the cooling (or heating) due to energy loss, and the second term is the heating due to straggling. The heating term (energy straggling) is given by [14, 15]

$$\frac{d(\Delta E_{\mu})_{\text{straggling}}^2}{ds} = 4\pi (r_e m_e c^2)^2 N_o \frac{Z}{A} \rho \gamma^2 \left(1 - \frac{\beta^2}{2}\right), \quad (3)$$

where N_o is Avogadro's number and ρ is the density.

The energy spread, and hence longitudinal emittance, is reduced by introducing a transverse variation in the absorber density or thickness (e.g. a wedge) at a location where there is dispersion (the transverse position is energy dependent). The concept is illustrated

in Fig. 2. The use of such wedges will reduce the energy spread and simultaneously increase the transverse emittance in the direction of the dispersion. Thus, longitudinal cooling is accomplished by the exchange of emittance between the longitudinal and transverse directions[16].

3.2 Ionization Cooling Channel

A complete muon ionization cooling channel might consist of 20 – 30 cooling stages. Each stage would yield about a factor of 2 in phase-space reduction and would consist of the following three components:

1. A low Z material in which energy is lost, enclosed in a focusing system to maintain a low β_{\perp} . There are two realizations of this currently under consideration:
 - A lattice consisting of axial high-field solenoids with alternating field directions. Liquid hydrogen absorbers are placed within the solenoids. (see Fig. 3).
 - Current carrying liquid lithium lenses. The magnetic field generated by the current provides the focusing, and the liquid lithium provides the absorber.
2. A lattice that includes bending magnets to generate dispersion, and wedges of absorber to lower the energies of the more energetic particles. This results in an exchange of longitudinal and transverse emittance.
3. A linac to restore the energy lost in the absorbers. In the alternating solenoid scheme the RF cells would be embedded within the matching section between the high-field solenoids, and would therefore be in a region in which the direction of the solenoidal field flips sign.

It is reasonable to use alternating solenoid lattices in the earlier cooling stages where the emittances are large. To obtain smaller transverse emittances as the muon beam travels down the cooling channel, the minimum β_{\perp} 's must decrease. This is accomplished by increasing the focusing fields and/or decreasing the muon momenta. Current carrying lithium lenses might therefore be used in the last few cooling stages to obtain much stronger radial focusing and minimize the final emittances.

Absorber

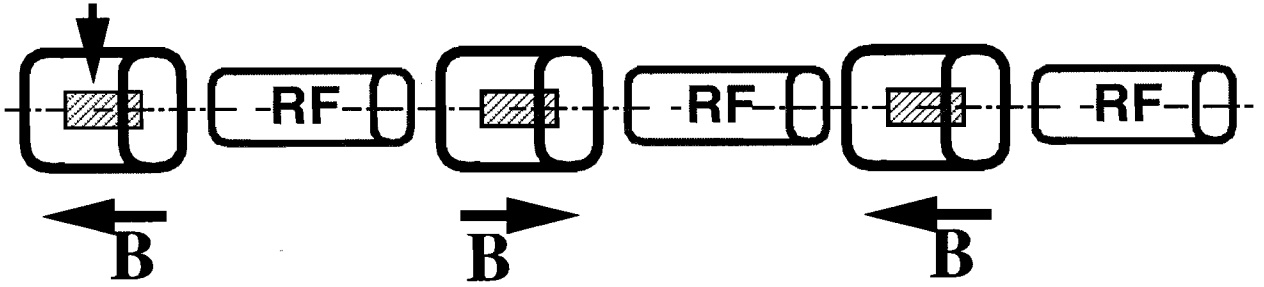


Figure 3: Conceptual schematic of an alternating solenoid ionization cooling lattice.

To test these ideas, and to explore the basic issues that must be addressed in the design of a complete cooling system, the performance of a “trial” cooling system has been calculated using analytic expressions for the beta functions, cooling and heating rates, and emittance acceptances. The trial system defined for this calculation was 750 m long, included a total re-acceleration of 4.7 GeV, and used LiH rather than liquid hydrogen absorbers. The fraction of muons that have not decayed and are available for acceleration at the end of the trial cooling system is calculated to be 55%. The calculated transverse emittance, longitudinal emittance, and beam energy are shown as a function of stage number in Fig. 4. In the first 15 stages the wedge sections are designed so that the longitudinal emittance is rapidly reduced, while the transverse emittance is decreased relatively slowly. The object is to reduce the bunch length, thus allowing the use of higher frequency and higher gradient RF in the re-acceleration linacs. In the next 10 stages, the emittances are reduced close to their asymptotic limits. In the last stages, the emittance is further reduced in current carrying lithium lenses. In order to obtain the required very low equilibrium transverse emittances, the focusing strength has been increased by allowing the energy to fall to 15 MeV. The use of energies this low results in a blow up of the longitudinal emittance, and at this stage no attempt is made to correct this by the use of dispersion and wedges.

The details of the lattices required for most of the cooling stages in the cooling channel are still being developed. Therefore, a complete alternating solenoid plus lithium lens cooling channel has not yet been simulated. However, simulations have been made of

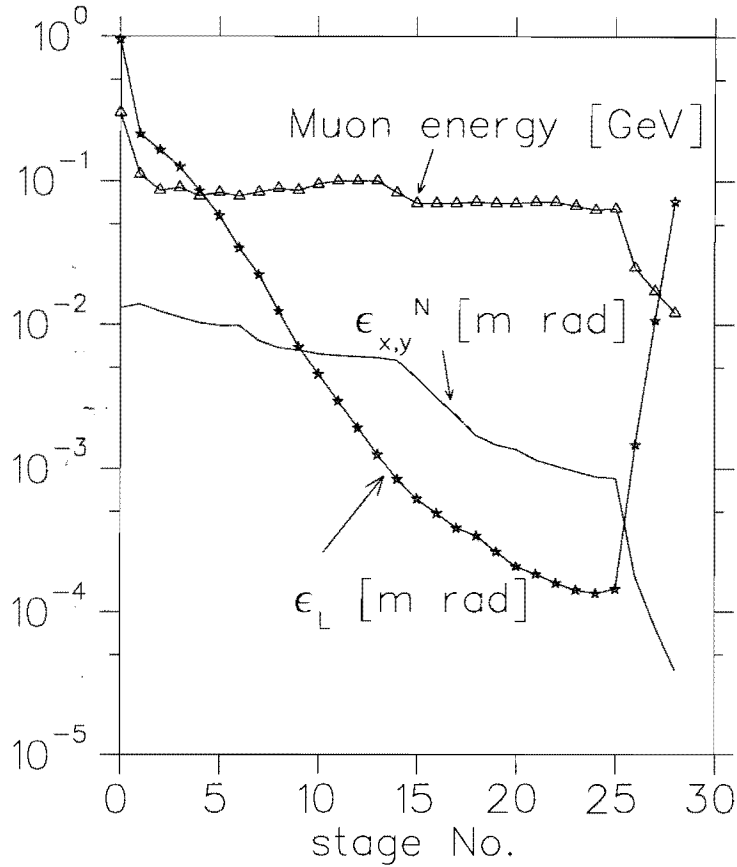


Figure 4: Calculated transverse emittance (ϵ_{\perp}), longitudinal emittance (ϵ_L), and beam energy shown as a function of stage number for the 750 m long cooling channel described in the text.

many of the individual components used in the cooling system, and cooling has been studied in different materials and with different beta functions. Furthermore, Monte Carlo calculations have been done to study wedge cooling using different beta functions and dispersions, and transverse cooling in lithium lenses has been simulated under a wide range of conditions[17, 19, 20, 21].

As an interesting example, in Fig. 5 results are shown from a simulation of a cooling channel constructed entirely from lithium lenses plus re-acceleration. The cooling channel consists of twelve 2 m long lithium lenses with re-acceleration at the end of each lens. The gradient is increased from lens to lens, following the reduction in beam size as the

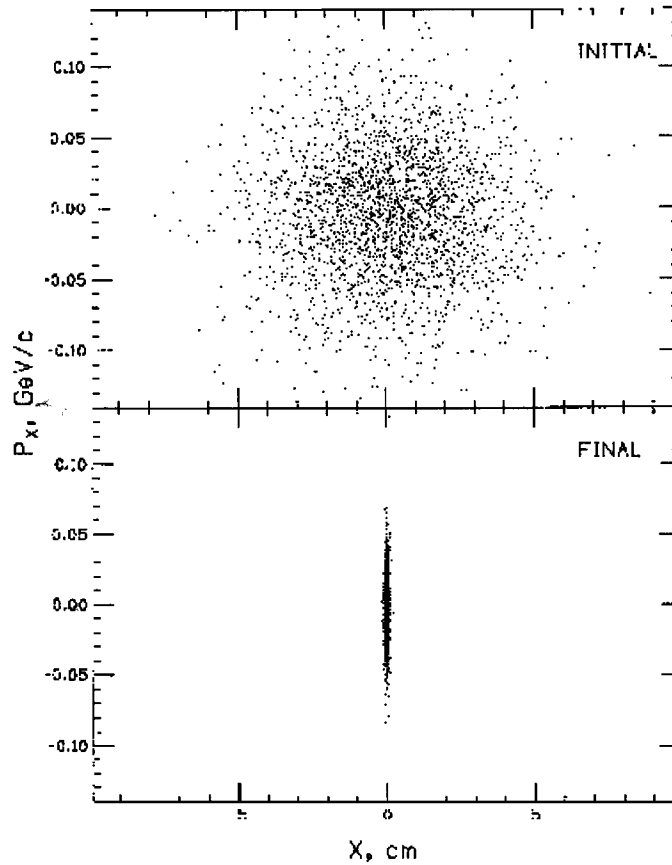


Figure 5: Results from a simulation of a lithium lens cooling channel.

beam is cooled. The calculation predicts a reduction in the normalized rms transverse emittance from $\sim 10000\pi$ mm-mrad to 80π mm-mrad. The parameters of the simulated cooling setup have not been optimized. However, the predicted final transverse emittance is already consistent with the requirements for a high-luminosity muon collider[22].

Although the initial simulations of a muon cooling scheme are encouraging, it should be noted that ionization cooling is a new technique that has not yet been demonstrated. In particular, there are practical challenges in designing lattices that can transport and focus the large initial emittances without exciting betatron oscillations that blow up the emittance and attenuate the beam. There are also potential problems with space charge

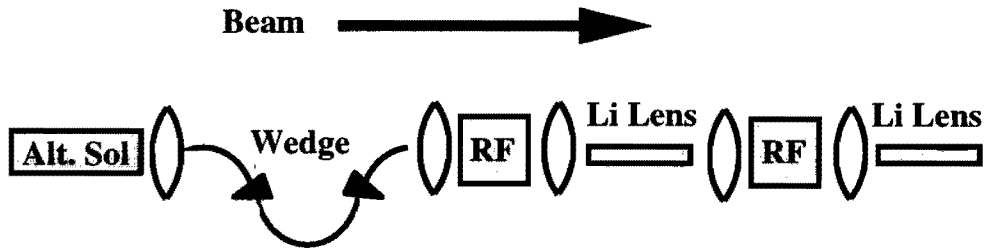


Figure 6: Schematic of the region of the ionization cooling channel in the neighborhood of the transition between the alternating solenoid and lithium lens cooling sections.

and wake fields. The theoretical design of an ionization cooling channel that overcomes these challenges is progressing.

4 Cooling Hardware Development

Our initial ionization cooling channel design studies have enabled us to identify the components needed for transverse cooling. We believe that, to understand the feasibility of building the ionization cooling channel needed for a high-luminosity muon collider, we must now design, construct, and test prototypes of the critical cooling channel components. This will require a vigorous R&D program. To succeed we must (i) develop cooling components that can achieve the operational parameters required for a real cooling channel, and (ii) demonstrate the cooling capability of a short prototype cooling channel using these components.

We propose to design, prototype, test, and optimize a section of the cooling channel in the neighborhood of the transition between the alternating solenoid and lithium lens cooling stages (Fig. 6). To carry out this R&D program we will require support for:

- (a) The development of an RF acceleration structure that can be used within the cooling channel.

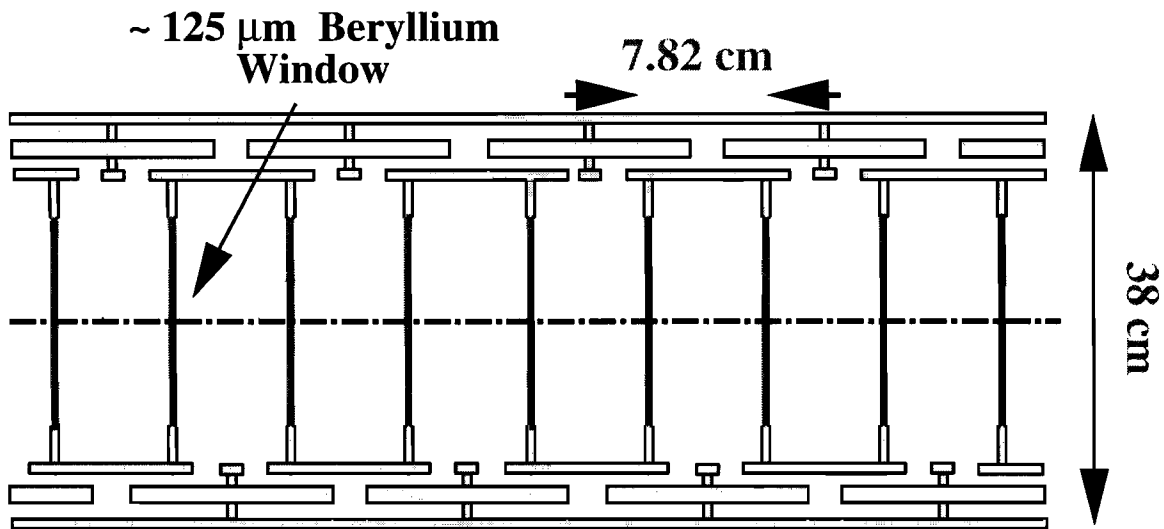


Figure 7: Interleaved $\pi/2$ accelerating structure.

- (b) The design, construction, and testing of a short section of an alternating solenoid cooling channel.
- (c) the design, construction, and testing of a wedge cooling section, and
- (d) the development of a long liquid lithium lens and a hybrid lens/wedge system suitable for the final cooling stages.

4.1 RF Accelerating Structure R&D

To minimize the length of the RF sections within the cooling channel, and hence minimize the decay losses during the cooling process, the maximum achievable accelerating gradients are needed. Fortunately, the penetrating properties of muons enable the use of accelerating structures in which thin conducting windows replace the normal open apertures between neighboring cells. The resulting structure is similar to the classic pillbox cavity, and yields an accelerating gradient on axis that approaches the peak gradient. The effective acceleration per cell is then approximately a factor of two larger than in a conventional open aperture cavity.

Initial design studies have focussed on the development of an RF cavity with the parameters listed in Table 1. These parameters have been chosen to correspond to the

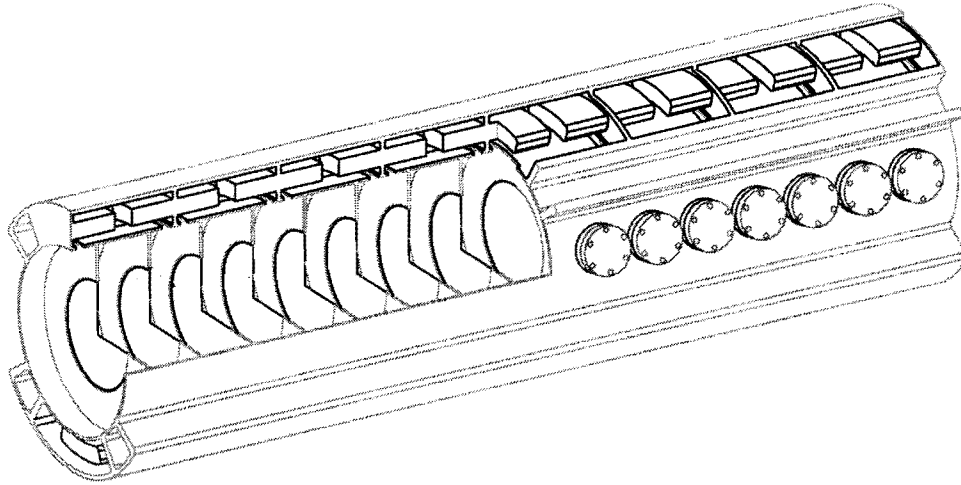


Figure 8: Preliminary design of an interleaved $\pi/2$ cavity module. The side ports enable access for multipactoring studies.

accelerating structure required for the cooling channel section that we propose to prototype and test, and which is described in section 4.2. The RF structure that is currently favored is shown in Fig. 7. The basic unit would be a 1.3 m long $\pi/2$ -mode standing wave cavity module (Fig. 8). Each module contains 16 cells that are interleaved to form two sub-systems, each consisting of an independently powered 8-cell side-coupled cavity. Details of the structure are shown in Fig 9. The individual cells are separated using windows made from 125 μm beryllium foils. Initial studies suggest that these foils will not contribute significantly to transverse heating of the beam due to Coulomb scattering.

The RF structure has been designed to operate at 805 MHz with a cell length of 7.82 cm, chosen so that the phase advance across each cell is $\pi/2$ rather than the standard phase advance of π per cell. This gives a better transit time factor, and hence yields a higher shunt impedance.

The RF modules must operate within the high-field superconducting solenoids of the

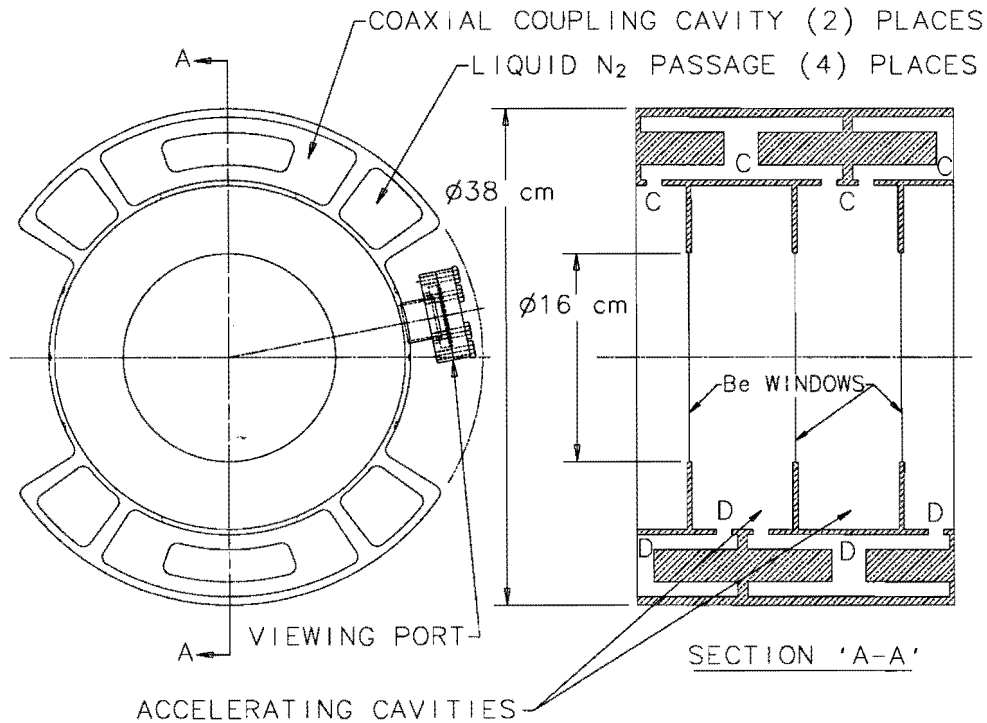


Figure 9: Details of the interleaved $\pi/2$ cavity.

cooling lattice. Although lattice design studies are still in progress, they are sufficiently advanced to enable the key RF parameters to be specified, and hence the R&D issues associated with the construction and operation of the RF accelerating structure to be identified:

- Operating temperature. Reducing the RF cavity operating temperature increases the cavity Q , and therefore increases the shunt impedance. This will reduce the total RF system cost. We plan to operate the cells at liquid nitrogen temperatures. Hence we must study, at liquid nitrogen temperatures, the Q of the cavity, the cavity coupling characteristics, and the operation of the proposed RF structure within the appropriate magnetic fields.
- Beryllium windows. The basic properties of beryllium at liquid nitrogen temperatures (resistivity, thermal conductivity, and thermal expansion coefficient) for commercially obtainable foils must be measured. A method of mounting beryllium

Table 1: Cavity parameters for the RF structure described in the text.

RF frequency [MHz]	805
Cell Length [cm]	7.82
Cavity Aperture [cm]	16
Cavity Outer Radius [cm]	19
Q/1000	2×22
Peak Axial Gradient [MV/m]	30
Shunt Impedance [$M\Omega/m$]	2×54
Z_t^2 [$M\Omega/m$]	2×44
Fill Time [μsec]	$3\tau = 26$
RF Peak Power [MW/m]	8.3
Avg Power (15Hz) [KW/m]	3.5

windows between the RF cells must be developed, and the mechanical stability of the windows and tunability of the cavities studied.

- Multipactoring. The presence of the windows within the cavity might give rise to electron discharge with resonant feedback (multipactoring). Multipactoring within a cavity with parallel beryllium walls separated by 7.82 cm must be studied within the appropriate magnetic fields.
- Accelerating gradients. Optimization to achieve the maximum practical accelerating gradients is desirable.

To address these R&D issues, we propose the following plan:

- (i) Material properties testing. A test setup has been constructed at BNL to measure the basic properties of beryllium samples at the appropriate RF frequencies and at liquid nitrogen temperatures. These measurements will begin shortly. Complementary DC measurements at liquid nitrogen temperatures will be performed at the University of Mississippi.
- (ii) Beryllium windows. A first design for the beryllium windows has been made at FNAL. It is hoped that fabrication, mechanical testing, and optimization of the window design will proceed soon.

Task	1998					1999					2000										
	3	4	5	6	7	8	9	10	11	12	1	2	3	4	5	6	7	8	9	10	11
Material props testing BNL RF tests Mississippi DC tests	█																				
Beryllium windows FNAL Design Fabrication Test Final window design Fabrication	█					█															
Low power test cavities LBL cavity design LBL cryogenic system LBL cavity assembly LBL Tests	█					█					█										
High power test cavity LBL Design LBL Fabrication LBL low power tests FNAL high power tests						█					█										
High power test setup LBL SC solenoid design LBL SC sol. fabrication LBL SC sol. tests FNAL Low level design FNAL Low level fabricatn FNAL Low level tests FNAL Vacuum system FNAL cryogenic design FNAL cryogenic fabricatn FNAL Klystron modulatr FNAL system assembly	█					█					█										

Figure 10: RF cavity development plan.

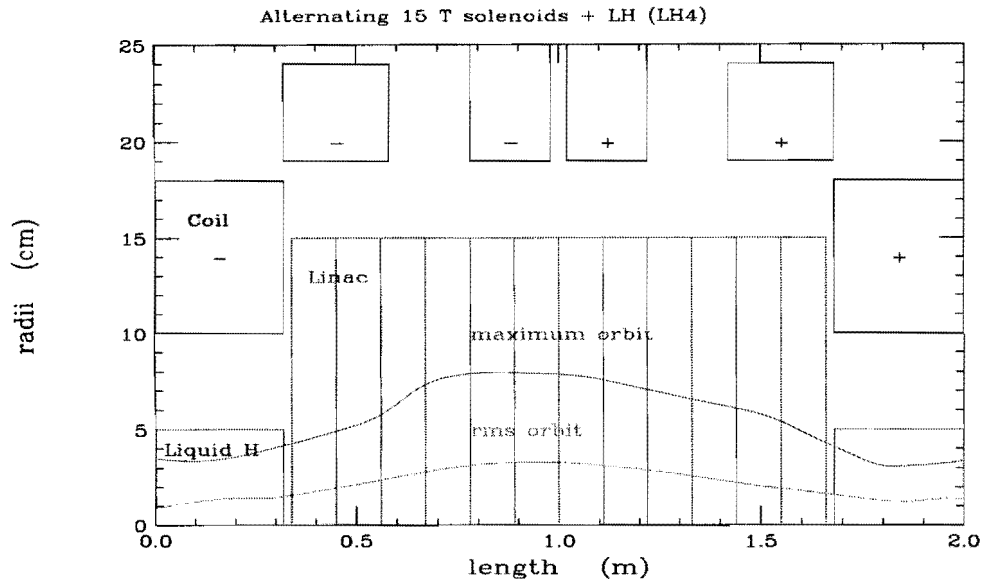


Figure 11: Schematic of a 2 m section (one period) of the alternating solenoid lattice described in the text.

- (iii) Low power test cavity. A 3-cell test cavity will be designed and fabricated at LBL and FNAL to test design ideas, and to study mechanical stability, cavity Q, and tunability at liquid nitrogen temperatures. The cavity will be tested at low power.
- (iv) High power test cavity. A 3-cell test cavity incorporating design modifications resulting from the low power test cavity studies will be fabricated at LBL. High power tests of this cavity will be made at FNAL in a 5.5 Tesla solenoidal field. The measurements would establish cavity operation, investigate multipactoring issues, and study cavity coupling characteristics.

A provisional schedule for this RF R&D program is shown in Fig. 10. At the end of 2 years our goal would be to have developed and tested the first prototype of the RF structure required for the transverse cooling section described in section 4.2. To meet this goal we will need a high-power RF test setup operational at FNAL in about 18 months from now. The high power test setup will require a 12 MW klystron, power supply plus pulse shaping network, a 5.5 T solenoid, and a shielded x-ray cave with inner dimensions of at least $(12 \times 40 \times 7.5) ft^3$.

Table 2: Preliminary parameters for a muon ionization cooling test section which corresponds to half of a transverse cooling stage in the neighborhood of the transition between the alternating solenoid and lithium lens cooling systems.

General Characteristics	
Lattice Period	2 m
Cooling section length	10 m
High Field Solenoids	
Peak Field	15 T
Warm Bore Radius	10 cm
Length	64 cm
Outer Matching Solenoids	
Peak Field	10 T
Warm Bore Radius	19 cm
Length	24 cm
Inner Field-Flip Solenoids	
Peak Field	5 T
Warm Bore Radius	19 cm
Length	18 cm
RF Characteristics	
Frequency	805 MHz
Peak Axial Field	30 MV/m
Cell length	7.82 cm
Cells / module	16
Absorber Characteristics	
Material	Liquid H_2
Minimum dE/dx	0.29 MeV/cm
Radiation Length	890 cm
Length / period	64 cm

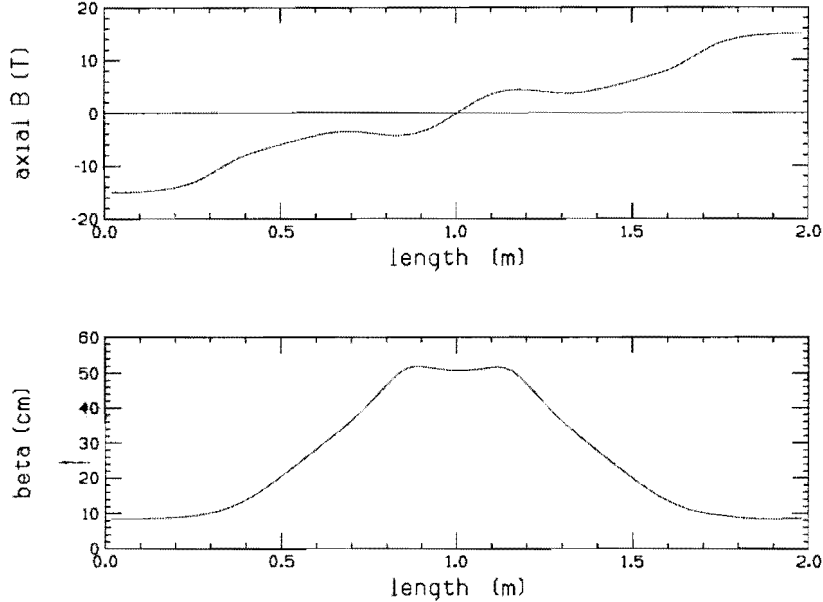


Figure 12: Variation of the solenoidal field strength (top plot), and the amplitude of the betatron oscillations (bottom plot), shown as a function of position along a 2 m (one period) section of the cooling lattice described in the text.

4.2 Transverse Cooling Channel Development

After developing a suitable RF accelerating structure, we propose to design, construct, and test a short section of an alternating solenoid transverse cooling channel. The test channel would be constructed from five 2 m long sub-sections. Figure 11 shows a schematic of one of these 2 m long sub-sections, which corresponds to one period of the cooling lattice. The 64 cm long, 10 cm diameter liquid hydrogen absorbers are interleaved between 1.3 m long RF modules which restore the longitudinal momentum of the beam particles as they traverse the periodic structure. These components are embedded in a solenoidal field which reverses direction within each period and has a maximum field strength of 15 T at the locations of the absorbers. The RF modules are within the solenoid matching sections in which the field direction is reversed. The variation of the field strength and the amplitude of the betatron oscillations along the length of the alternating solenoid lattice is shown in Fig. 12, and the parameters describing the test cooling section are summarized in Table 2. A GEANT simulation of muons traversing a section of the cooling test channel is shown in Fig. 13.

The test cooling section corresponds to about one half of a transverse cooling stage lo-

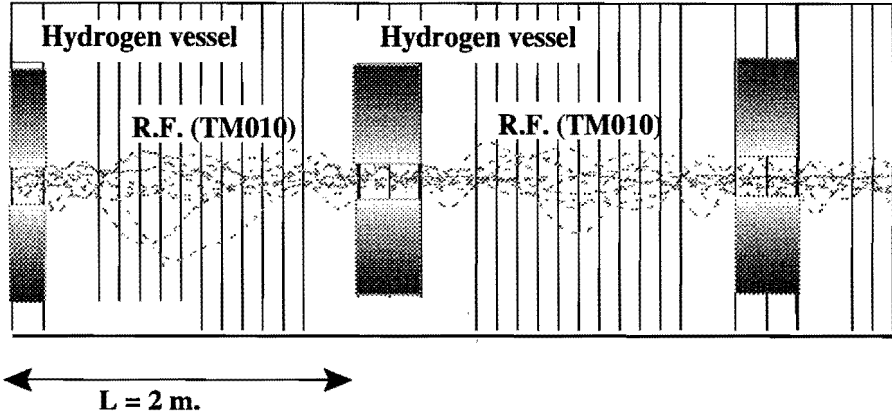


Figure 13: GEANT simulation of muons traversing a section of the alternating solenoid cooling channel discussed in the text.

cated towards the end of the alternating solenoid cooling channel, just before the transition to lithium lens (or very-high field solenoid) cooling. We have simulated the performance of this cooling stage using the ICOOL program, which is described in Section 5.5. In the simulation, muons are generated at the upstream end of the cooling section and are tracked through the cooling lattice. The generated population of muons has the chosen central value of momentum (186 MeV/c), and the appropriate transverse- and longitudinal-emittances ($\epsilon_T = 1400\pi$ mm mr and $\epsilon_L = 1000\pi$ dp/p mm). In addition, the generated muons have the appropriate angular momentum corresponding to the starting axial magnetic field, and the population of muons were generated with (i) the naturally occurring correlation between momentum and the square of the betatron amplitude that ensures that the forward velocities are independent of amplitude, and (ii) a distortion of the longitudinal bunch distribution that reflects the asymmetric nature of the effective RF bucket.

Results from the simulation are shown in Figs. 14–16. The average beam momentum falls as the beam traverses the liquid hydrogen absorbers, and increases as it traverses the RF modules (Fig. 14a), whilst the angular momentum of the muons oscillates as the muons pass through positive and negative values in the reversing axial fields (Fig. 14b). The evolution of the beam envelope as the beam traverses the cooling stage is shown in Fig. 15,

Table 3: Initial and final beam parameters for a 22 m long transverse cooling stage.

		initial	final	factor
Transverse Emittance	π mm mrad	1400	650	0.46
Longitudinal Emittance	π mm mrad	1000	2040	2.04
6D emittance	$10^{-12} \times (\pi \text{ m rad})^3$	1990	880	0.46
rms beam size in hydrogen	cm	0.8	0.55	0.69
rms beam size in linac	cm	2.0	1.4	0.70
max beam rad in linac	cm	7.0	7.0	1.0
rms bunch length	cm	1.5	2.2	1.5
max bunch full width	cm	13	19	1.5
rms dp/p	%	3.8	5.6	1.5

Table 4: List of cooling components needed for the proposed transverse cooling test section.

4	High field solenoids (64 cm long)
2	High field solenoids (32 cm long)
10	Outer matching solenoids
10	Inner (field flip) solenoids
5	RF modules
5	12 MW klystrons
5	klystron power supplies
5	pulse forming networks
5	Liquid H_2 absorber modules

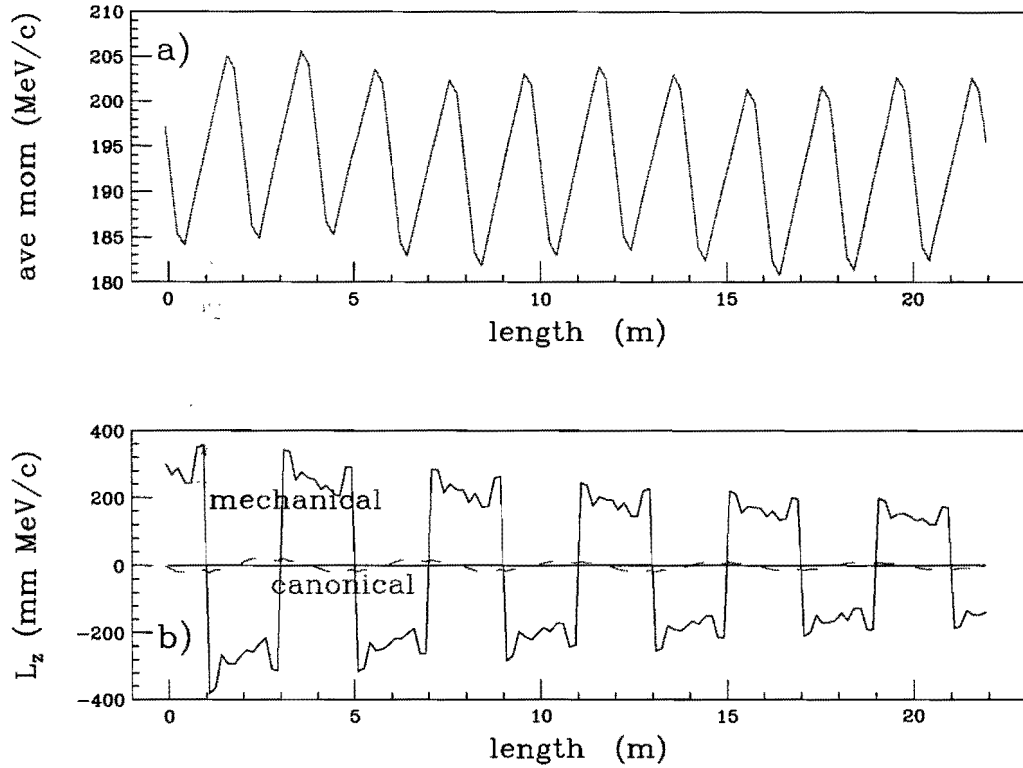


Figure 14: Simulation results for the average (a) muon momentum, and (b) mechanical (solid curve) and canonical (broken curve) muon angular momentum, shown as a function of distance along the cooling stage described in the text.

together with the rms momentum spread calculated after correcting for the amplitude-momentum correlation, and the rms bunch length. Note that the momentum spread slowly increases due to straggling and the adverse dependence of the dE/dx losses with muon energy. Finally, the evolution of the transverse-, longitudinal-, and 6-dimensional-emittances as the beam traverses the 22 m long cooling stage is shown in Fig. 16, and the results are summarized in Table 4.2. The transverse emittance falls by a factor of about 2, whilst the longitudinal emittance increases by about a factor of 2. Hence, the 6-dimensional emittance is decreased by about a factor of 2. Note that the simulation predicts that the 10 m cooling test section will decrease the 6-dimensional emittance by about a factor of 0.7.

The ICOOL simulations performed so far do not include the effect of space charge or

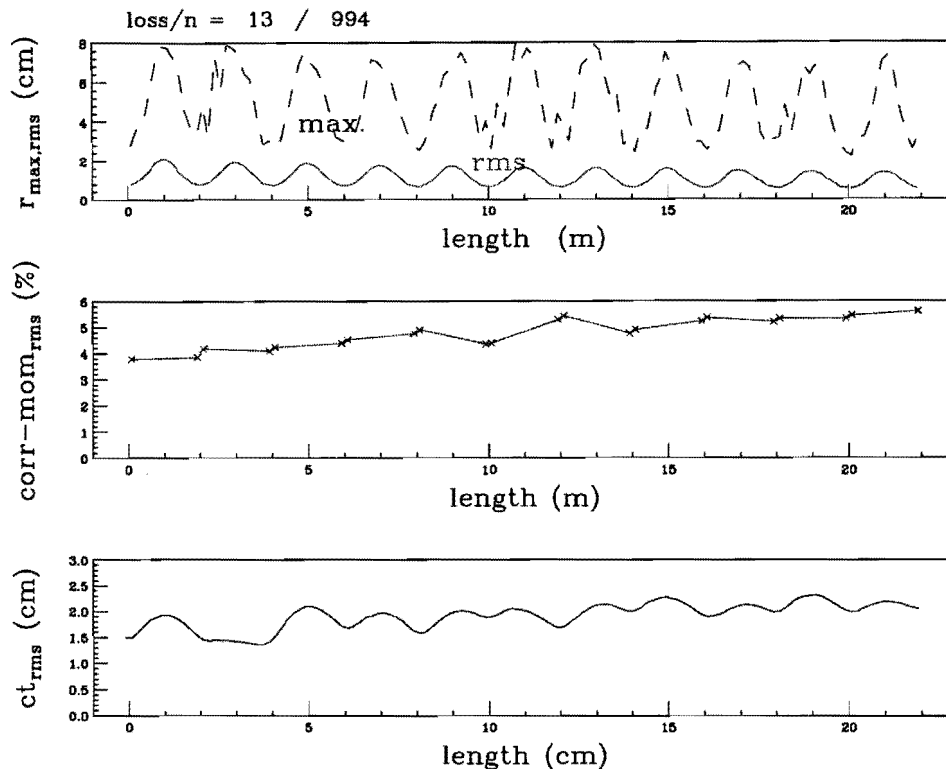


Figure 15: Simulation results for (a) the rms and maximum beam radii, (b) the rms momentum spread after correcting for the amplitude-momentum correlation, and (c) the rms bunch length, shown as a function of distance along the cooling stage described in the text.

wake fields. Work on including these collective effects in the calculation is in progress. Analytic calculations indicate that, for the later cooling stages in a muon collider cooling channel, space charge and wake field effects may be significant, but not overwhelming. A complete simulation including these effects must be performed to check that they do not introduce significant problems in the cooling channel.

The main cooling channel components needed to construct a 10 m long alternating solenoid test section are listed in Table 4. We are proposing to measure the performance of this test section in a muon beam with the appropriate beam momentum (~ 187 MeV/c). The beam test would be designed to:

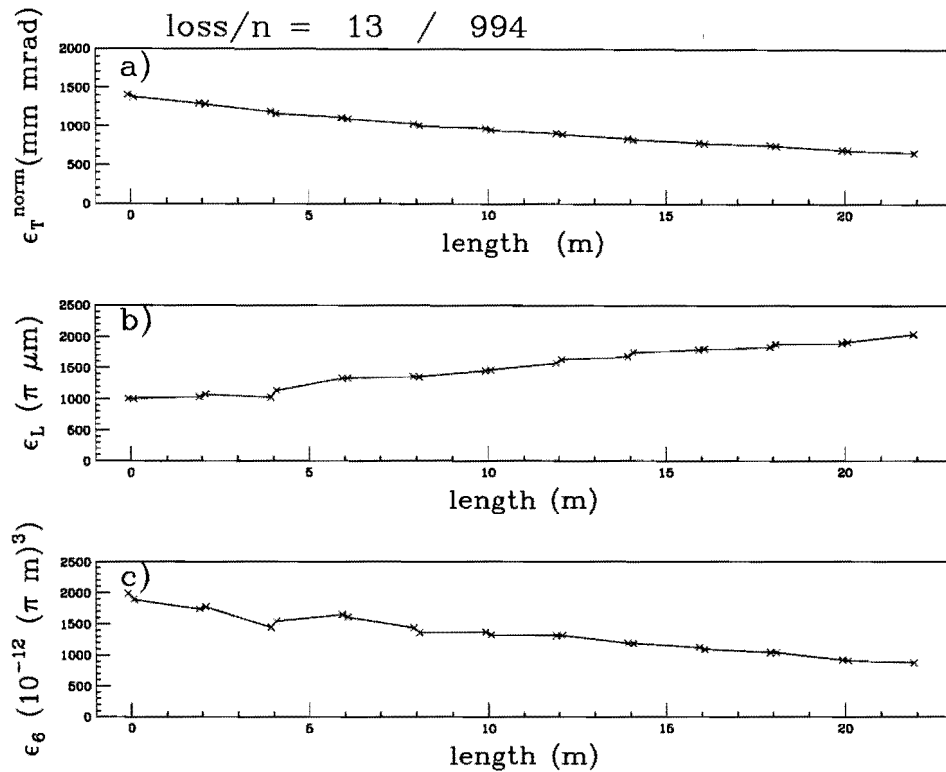


Figure 16: Results from a simulation of an alternating solenoid transverse cooling stage described in the text. Shown as a function of distance along the cooling stage is the evolution of (a) the transverse emittance, (b) the longitudinal emittance, and (c) total 6-dimensional emittance.

- (i) Demonstrate the cooling capability of the test section in a low intensity muon beam.
- (ii) Test the simulation tools used to design the cooling channel.
- (iii) Study the non-decay loss of muons traversing the cooling section.
- (iv) Study correlations between the positions of muons in 6-dimensional phase space at the input and output of the cooling channel, and hence investigate further optimization of the cooling scheme.

To prepare for the beam test we need to first finalize the design of the cooling test section, and complete the RF R&D described in the previous section. Following this we

Task	YEAR					
	1998	1999	2000	2001	2002	2003
RF Development Cavity development	████████████████████					
First Test Section (2m) 1.3 m RF module design 1st module fabrication 1st RF module test Solenoid design Solenoid fabrication LH2 module design LH2 module fabrication Assembly and bench test		██████████	██████████ ██████████	██████████ ██████████		
Test Channel (10m) RF module production Klystrons, power supplies Solenoid production LH2 module production Assembly and bench test				██████████ ██████████	██████████ ██████████	██████████

Figure 17: Alternating solenoid test channel construction plan.

propose to prototype and test a 1.3 m long RF module, and then construct five of these modules for a 10 m transverse cooling section. We would also need to build the vacuum, cryogenic, and RF subsystems (klystrons, power supplies, pulse forming networks) needed to operate the RF modules, and design and construct the solenoids, and liquid hydrogen absorber systems. A preliminary plan for the cooling channel preparation is shown in Fig. 17. We believe that the first section of the test channel would be ready for beam tests in early 2002. The full 10 m cooling section would be ready for beam tests in 2003.

4.3 Wedge Cooling Channel Development

Initial design studies for a wedge cooling section are in progress. To reduce the longitudinal emittance of the beam (at the expense of the transverse emittance) wedge cooling requires dispersion in a large acceptance channel, followed by one or more low Z wedge absorbers. In our initial design study we have considered a wedge cooling system within a continuous 3.5 T solenoidal channel. Dispersion is generated by bending the solenoid. In a bent

LONGITUDINAL COOLING

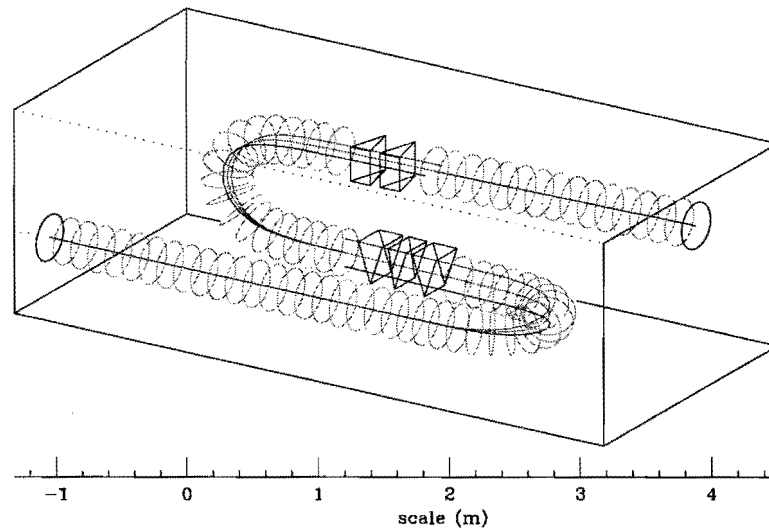


Figure 18: Schematic of the bent solenoid longitudinal emittance exchange section used in the initial wedge cooling design study.

solenoid there is a drift perpendicular to the bend that is proportional to the particle's momentum (the "curvature drift effect"). In the wedge cooling lattice being studied, a dipole field is superimposed on the solenoidal field over the bend region, so that the curvature drift effect is canceled for particles having the reference momentum. Particles above (below) the reference momentum are then drifted up (down), giving the required dispersion. Longitudinal cooling (by emittance exchange) is accomplished by introducing liquid hydrogen wedges downstream of the bend so that the higher momentum particles pass through more material than the lower momentum ones. This removes the dispersion and reduces the momentum spread.

After one bend and one set of wedges, the beam has an asymmetric cross section. Symmetry is restored by a second bend and wedge system that is rotated by 90 degrees with respect to the first system. The geometry is illustrated in Fig. 18 which shows a representation of the two bends and associated wedges. In our preliminary design study the total solenoid length is 8.5 m, with a beam tube outside diameter of 20 cm, and minimum bend radii of 34 cm. The bend curvatures correspond to the trajectory of a reference particle propagating on axis down the channel through the superimposed transverse dipole fields. Note that the curvature changes at the two ends of the bend sections are gradual, the shape being chosen to minimize emittance growth.

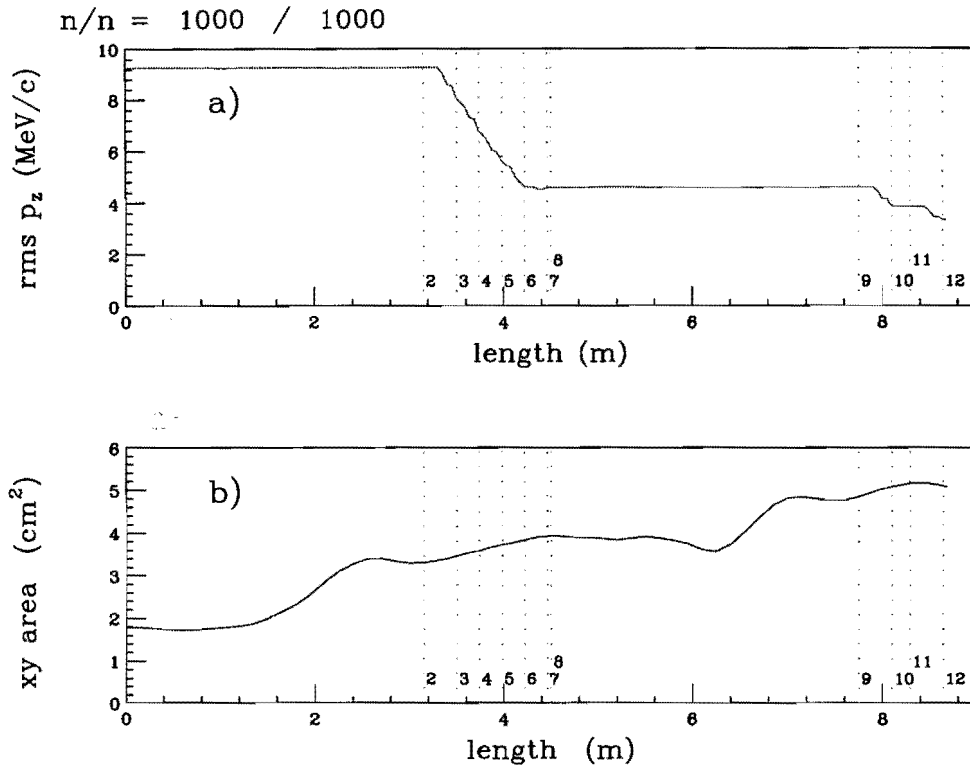


Figure 19: Results from a simulation of the wedge cooling cooling stage described in the text. Shown as a function of distance along the cooling stage is the evolution of (a) the longitudinal momentum spread, and (b) the transverse beam area. The liquid hydrogen wedges are in the regions 2-6 and 9-11.

The performance of the wedge cooling channel shown in Fig. 18 has been simulated using the ICOOL program. In our initial study, the containment windows of the liquid hydrogen absorber vessels have not been included in the simulation, and space charge and wake field effects have not been taken into account. The simulations show that the beam profile rotates as the beam passes down the solenoid channel, introducing x-y correlations in the middle of the cooling section which are removed at the end by additional rotations of the axes. In addition, although the actual angular momentum of the beam remains approximately constant throughout the channel, the canonical angular momentum increases in the region in which the dispersion is increasing the radial size of the beam. In a real wedge cooling system, this increase in canonical angular momentum

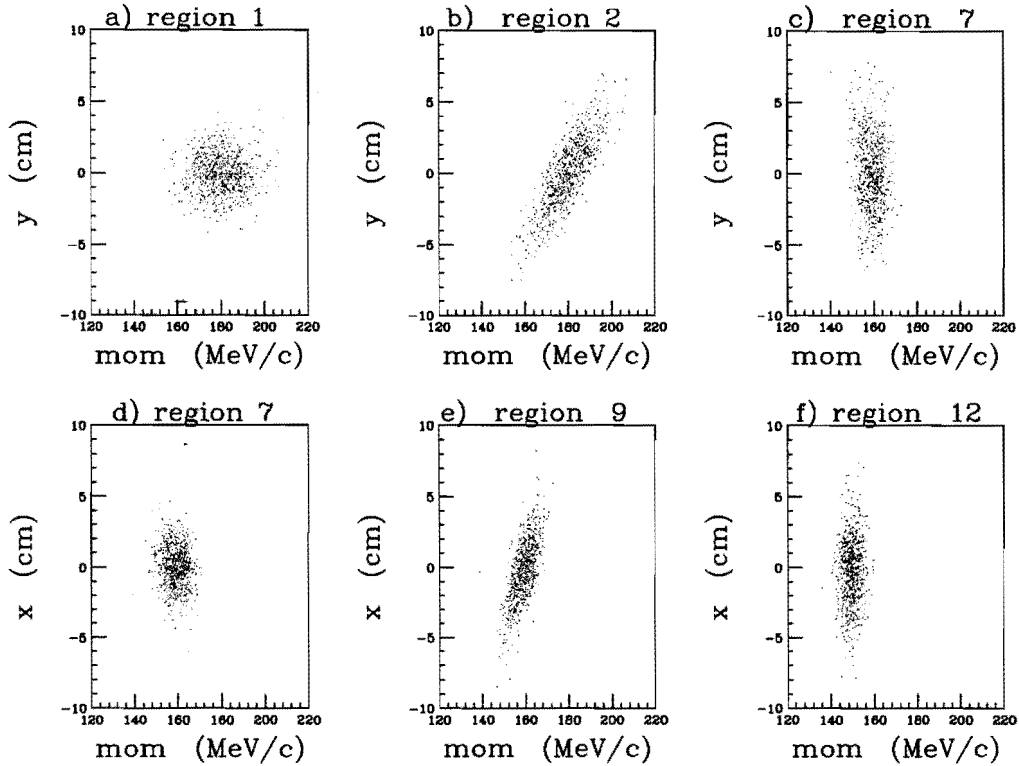


Figure 20: Results from a simulation of the wedge cooling cooling stage described in the text. Shown as a function of distance along the cooling stage is the evolution of the beam in the (y, p_z) -plane (a) at the start, (b) after the first bend, and (c) after the first wedges. Also shown is the evolution of the beam in the (x, p_z) -plane (d) after the first wedges, (e) after the second bend, and (f) at the end of the channel.

would be removed by a field reversal section followed by transverse cooling. However, in our initial study the excess canonical angular momentum was removed just before the end of the cooling section using a simple matrix. Thus the detailed performance of a wedge cooling channel is complicated, and all of the effects described above require further study.

Figure 19a shows the simulated longitudinal momentum spread as a function of length down the wedge cooling channel. The rms momentum spread decreases from an initial value of approximately 5%, to a final value of approximately 2.2%. At the same time, since this is an emittance exchange, the transverse beam area grows (Fig. 19b). Note that the beam area increases not only in the regions of the bends (region 1 and 8), but also in

Table 5: Wedge cooling simulation results. Initial and calculated final beam parameters for the wedge cooling channel described in the text.

		initial	final	factor
σ_p	MeV/c	9.26	3.35	0.36
Ave. Momentum	MeV/c	180	150	0.83
Transverse size	cm	1.33	2.26	1.70
Transverse Momentum	MeV/c	6.84	7.84	1.15
Transverse Emittance	π mm mrad	870	1694	1.95
$\text{Emit}_{trans}^2 \times dp_{long}$	$(\pi \text{ m mrad})^2 \text{ MeV/c}$	7.0	9.6	1.37

the regions of the wedges (2-6 and 9-11). This is probably due to failures in matching that have yet to be understood. The evolution of the beam in the (x,p_x) - and (y,p_y) -planes is shown in Fig. 20. The dispersion introduced by the first bend (region 2) is clearly seen to be removed by the liquid hydrogen wedges (region 7). The second bend (region 9) introduces dispersion in the orthogonal co-ordinate, which is removed by the second wedges (region 12). The momentum spread is clearly decreased at the end of the wedge cooling channel, at the expense of an increase in transverse emittance.

The initial and final beam parameters from our preliminary wedge cooling study are summarized in Table 5. The beam momentum spread is reduced by almost a factor of 3. These initial results are encouraging, although more work is required to understand and reduce the 5-dimensional emittance increase of 37%, which we believe arises from mis-matching, and indicates a need for further optimization of the design. In the next step we must also include RF modules in the simulation to allow the evolution of the 6-dimensional emittance to be studied.

We anticipate that in the next year our wedge cooling design studies would have advanced to the point where we can specify the required performance parameters for a prototype wedge cooling system. A full design of the prototype system might begin in 2000, with a completed wedge test channel ready for measurements at a beam cooling test facility in 2003.

4.4 Lithium Lens Research and Development

Lithium rods with surface fields of 10–18 T were developed at Novosibirsk (BINP), and have been operated with high reliability as focusing elements at FNAL and CERN [23, 24, 25, 26]. Although these lithium lenses have many similar properties to those required for ionization cooling, there are some key differences which will require lithium lens technology to be extended to its practical limits. In particular:

- Ionization cooling requires much longer lenses than previously developed. Lenses with lengths of the order of a meter are required to maximize the amount of cooling in a single absorber and hence minimize the number of transitions from absorber to absorber.
- The muon collider repetition rate will require the lithium lenses to operate at 15 Hz. The resulting thermal load on a solid lithium lens would increase its temperature to the melting point ($T_{melt} = 186^{\circ}\text{C}$). It is therefore desirable to operate with lithium in the liquid phase, flowing through the lens for cooling. Note that, since lithium is more compressible in the liquid phase, liquid lithium lenses are expected to be more durable than solid rods. The superior thermal and mechanical properties of a liquid lens are expected to facilitate longer lens lifetimes and permit higher achievable maximum surface fields.
- To minimize the final emittances, the maximum radial focusing, and hence the maximum surface fields are required. It is hoped that liquid lithium columns can be used to raise the surface field to 20–25 T.

The parameters of the lithium lenses needed for a muon ionization cooling channel are listed in Table 6.

Prototype liquid lithium lenses have been developed at Novosibirsk [27]. Currently a contract between BINP and Fermilab exists for the development of a high-field 15 cm long liquid lithium lens for antiproton collection. The designs for the lens and liquid metal pump were reviewed and approved in March 1998. Construction of these items is expected to be completed in December 1998. The power supply needed for the lens is currently being designed and will be built in 1999. Bench testing of the lens is foreseen at BINP in 1999, with transport of the lens system to Fermilab in 2000. As the liquid

LITHIUM CURRENT CARRYING COOLING ROD

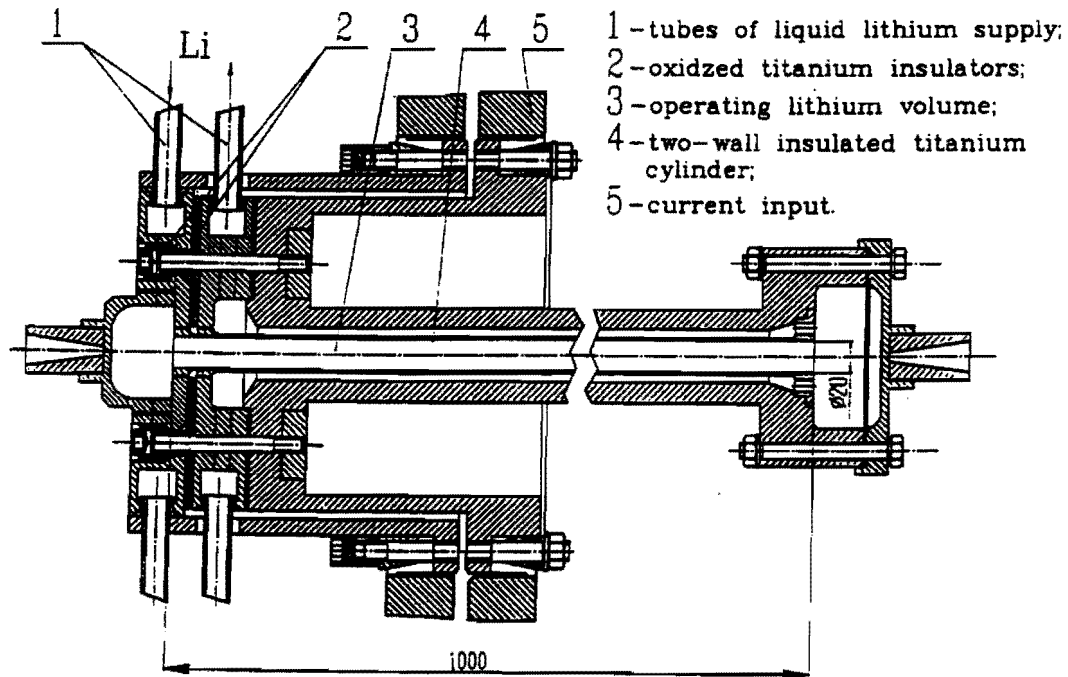


Figure 21: Schematic of a 1 m long liquid lithium lens with a surface field of 10 T designed by Silvestrov to be used for ionization cooling.

lithium lens technology is established it will be transferred to Fermilab, where further development can be pursued.

The liquid lithium lens R&D effort will need to be expanded to develop the longer lenses needed for ionization cooling. Figure 21 shows a schematic of a 1 m long lithium lens designed at BINP by Silvestrov to be used for ionization cooling. The lens uses liquid lithium, and has a radius of 1 cm and a surface field of 10 T. A collaboration with BINP and Argonne National Laboratory to develop a similar 1 m long lens for ionization cooling is being explored. A power supply that is suitable for this long liquid lithium lens is available at CERN. This power supply consists of a 22 mF capacitor bank which is charged to 4.2 kV, yielding a stored energy of 200 kJ which can be coupled to the lithium lens with a transformer [28]. The unit is modular and can be modified to suit the

particular current and voltage requirements of a given lens. It is hoped to transport the CERN power supply to Fermilab for lens bench-testing and operation.

A second lens with a higher surface field would be designed and constructed to enable a complete cooling step to be tested, including re-acceleration after the first lens and matching into the second lens. Simulations indicate that a single 1 m long lens would cool the normalized rms transverse emittance from 1000π mm-mrad to 670π mm-mrad, and cool the six-dimensional emittance to 60% of its initial value. Addition of a second lens is predicted to cool the normalized rms transverse emittance to $\sim 500\pi$ mm-mrad, reducing the six-dimensional emittance to 40% of its initial value. The lens-RF-lens system would be tested in a muon beam of the appropriate momentum (~ 260 MeV/c).

In addition to the development and testing of the first Silvestrov-type long liquid lithium lenses, we would propose to extend the lens R&D to try to maximize the surface fields, and to study other geometries and the inclusion of other materials. Note that material choices are limited since a cooling lens must be both a good conductor and be constructed from low-Z material to minimize multiple scattering. A possible alternative to lithium is beryllium ($Z = 4$) which has a higher density. However, beryllium rods may be too brittle. Boron and carbon might also be integrated into the design, and designs with alloyed materials might be developed. These higher density solid materials may be needed for the longitudinal (wedge) cooling. Designs which integrate the active lens with wedge absorbers have been initiated.

The proposed lithium lens R&D program consists of the following:

- Design, construction, and bench testing of the first 1 m long liquid lithium lens of design similar to the one developed by Silvestrov. The lens should be tested with at least 10^6 pulses to assess its lifetime.
- Design, construction, and testing of a second 1 m long liquid lithium lens with the highest achievable surface field.
- Measurement of the performance of a lens-RF-lens cooling system in a low energy muon beam, using the two lenses that would have been built.
- Development and testing of a hybrid lens/wedge system.

Table 6: Lithium lens parameters for a muon ionization cooling channel.

B (T)	B' (T/m)	Radius (cm)	Length (m)	I (MA)	$\tau(\delta = 0.7r)$ μs	$\Delta T/\text{pulse}$ ($^{\circ}\text{C}$)
10	1000	1.0	1	0.5	1000	78
15	3000	0.5	1	0.375	250	177
20	8000	0.25	1	0.25	63	316
20	16000	0.125	1	0.125	15	303

A tentative schedule for the development of long liquid lithium lenses for ionization cooling is shown in Fig. 22. We estimate that the lens-RF-lens system would be available for beam tests in 2003, and a hybrid wedge/lens system would be ready for beam measurements at the beginning of 2004.

5 Ionization Cooling Test Facility

The experiments required to demonstrate ionization cooling and to develop and optimize the cooling hardware described in the previous sections will not be trivial. They will require an ionization cooling test facility with the following capabilities:

- Injection of single muons with momenta in the range 100 - 300 MeV/c into a test cooling setup initially of length ~ 30 m, and eventually extending up to ~ 50 m.
- Measurement of the six-dimensional phase-space volume occupied by the populations of the incoming and outgoing muons with a precision of a few %.
- Measurement of the non-decay loss of muons traversing the cooling setup with a precision corresponding to $O(10\%)$ for a full cooling stage. Since the non-decay losses are expected to be $\sim 1\%$, each measurement will require $O(10^4)$ muons within the phase-space acceptance of the cooling apparatus.

To provide these capabilities the facility will need to have a low energy muon beam-line, the infrastructure to operate the cooling prototypes to be tested (services, shielding, overhead crane coverage, refrigerants for superconducting magnets, RF power for accelerating cavities including modulators, klystrons, etc), and instrumentation to identify

Task	YEAR					
	1998	1999	2000	2001	2002	2003
Pbar Source lens R&D	█					
First 1m Lens Design lens Commision power supply Fabricate lens Bench test lens		█ █	█	█		
Second Lens Design high-gradient lens Design lens power supply Fabricate lens Fabricate power supply Bench test lens Beam test lens-RF-lens			█	█ █	█ █	█ █
Wedge/lens hybrid Design Fabricate Bench Test				█ █	█ █	█

Figure 22: Tentative long liquid lithium lens development plan.

incoming and outgoing muons and determine their positions, directions, momenta, and their entrance and exit times with respect to the RF acceleration cycle.

Work on an initial design of the required facility is proceeding. In the following subsection we describe our current understanding of the beam requirements and candidate beamlines for satisfying our requirements. The remaining subsections then describe the measurements to be made and the instrumentation that will be required.

5.1 Low Energy Muon Beamline

The prototype cooling hardware tests described in the previous sections require a high purity (> 99%) tagged muon beam with a central momentum of 187 MeV/c for the

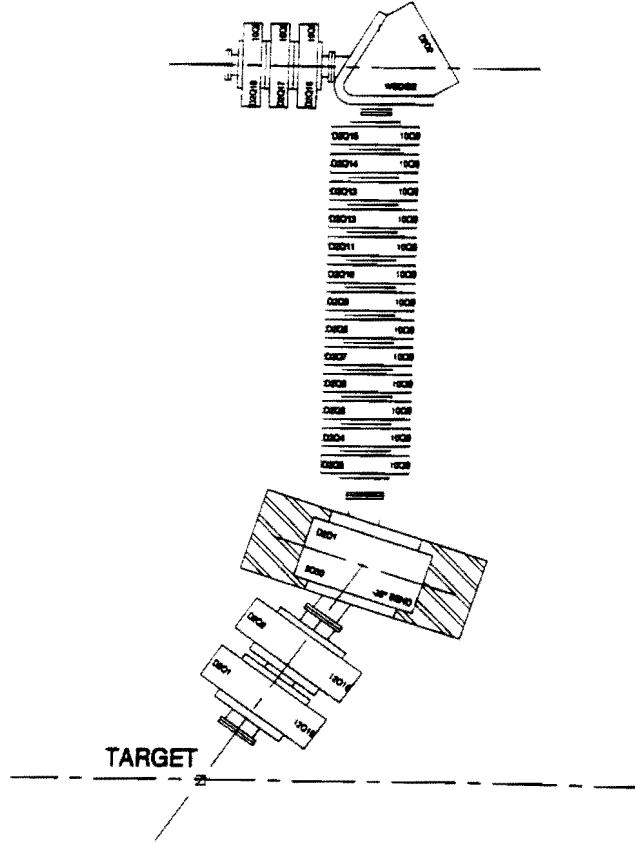


Figure 23: Schematic of the existing D2 muon beamline at BNL.

alternating solenoid cooling channel measurements and 260 MeV/c for the lithium lens measurements. Anticipating that as the cooling hardware R&D program advances we will require some flexibility in choosing the momenta of the muons used for the measurements, the cooling test facility beamline will need to provide muons with central momenta that can be chosen in the range $\sim 100 - 300$ MeV/c. A small spread in beam momentum is also required. Existing low energy muon beamline parameters suggest that $\Delta p/p = 5\%$ is a reasonable goal. Finally, we require a normalized rms transverse beam emittance of $\sim 1300\pi$ mm-mr to provide an appropriate test of the cooling hardware.

Existing low energy muon beamlines have been constructed using large aperture quadrupole decay channels with large angle bending dipoles to suppress backgrounds. Two interesting examples are:

- (i) The decommissioned MEGA beamline at LAMPF. Most of the magnets from this beamline are in storage and may be available, including nine 12 inch aperture 65 cm

long quadrupoles, eleven 12 inch aperture 50 cm long quadrupoles, and three 6.1 KG field 105 cm long bending magnets.

- (ii) The D2 beamline at BNL (Fig. 23), which is assembled in the backward-decay configuration. The beamline consists of a pion collection part, a pion decay part, and a muon matching part, each separated by bending magnets. Since the backwards muons have about half the momentum of the undecayed pions, this configuration produces a muon beam with very small pion contamination. The major background particles are electrons. The D2 line uses a slow extracted beam from the AGS. In its present configuration it is limited to muons with less than 150 MeV/c momentum. The available muon flux has been measured to be 2×10^6 per 10^{13} protons on target. The beamline could be modified to produce a higher energy muon beam by replacing the last dipole and using higher current cables from the power supplies.

These beamlines are not currently used. It is therefore conceivable that some or all of the magnets may be available to build a new low energy beamline for ionization cooling tests at Fermilab.

5.2 Beam Requirements and Muon Rates

Beamline design studies are in progress using the general characteristics of the BNL D2 and LANL MEGA beamline magnets, with the pion production target located either at the end of a 120 GeV/c Main Injector proton beamline or at the end of a new 8 GeV/c Booster proton beamline. To understand the number of primary protons required on the pion production target per measurement, and the effect of the proton bunch structure on the measurements, it should be noted that:

- (i) Useful cooling only occurs for beam particles arriving at the right phase in the re-acceleration RF cycle (about 5% of the RF period). With an RF frequency of 805 MHz, the RF acceptance is therefore about 62 ps in every 1.24 ns cycle.
- (ii) To correctly identify the incoming and outgoing muons traversing the experiment we will require the instantaneous rate to be modest. We currently believe that we will be able to correctly reconstruct the muon tracks provided there are no more than

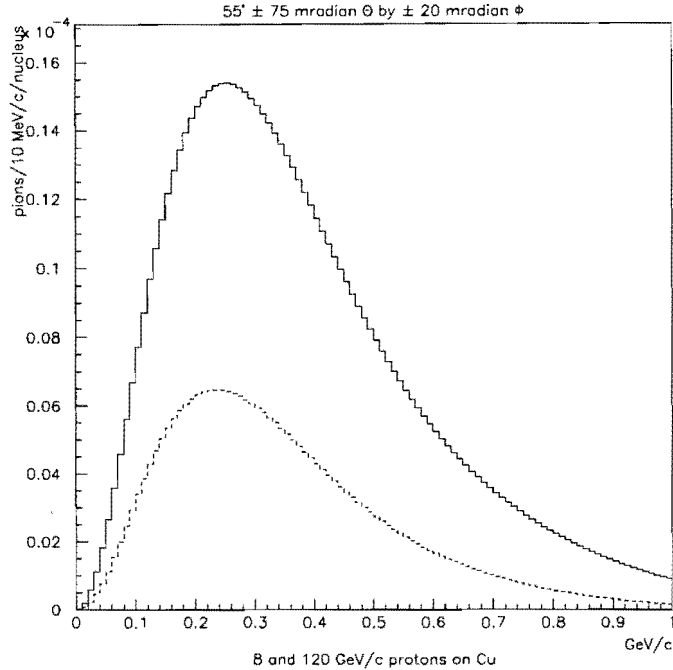


Figure 24: MARS calculation of the π^+ production rates for 8 GeV/c (broken curve) and 120 GeV/c (solid curve) protons incident on a copper target.

~ 10 tracks per $6 \mu\text{s}$ interval traversing the instrumentation, and the times between the tracks are longer than $\sim 5 \text{ ns}$.

Our initial low energy muon beamline studies use calculated pion production rates (Fig. 24), together with a simulation of the muon channel acceptance for a channel that consists of a quadrupole collection stage to define the desired beam acceptance, two dipole bends for momentum selection, a FODO channel between the dipoles to define the pion decay space, and a final quadrupole stage to match into the experiment. Bend angles of 35° and 90° have been chosen to control muon and hadron backgrounds. The large angles combined with appropriate collimation also provide the momentum acceptance required by the experiment. The beamline configuration we have studied is designed to collect positive muons from forward pion decays with the pions collected from the production target at 55° . This angle was chosen to correspond to the Cocconi angle for 300 MeV/c positive pions, which minimizes the backgrounds from higher momentum particles (Fig. 25).

Our initial beamline studies are summarized in the following sub-sections. We note that our beam studies are preliminary and more work must be done to determine the

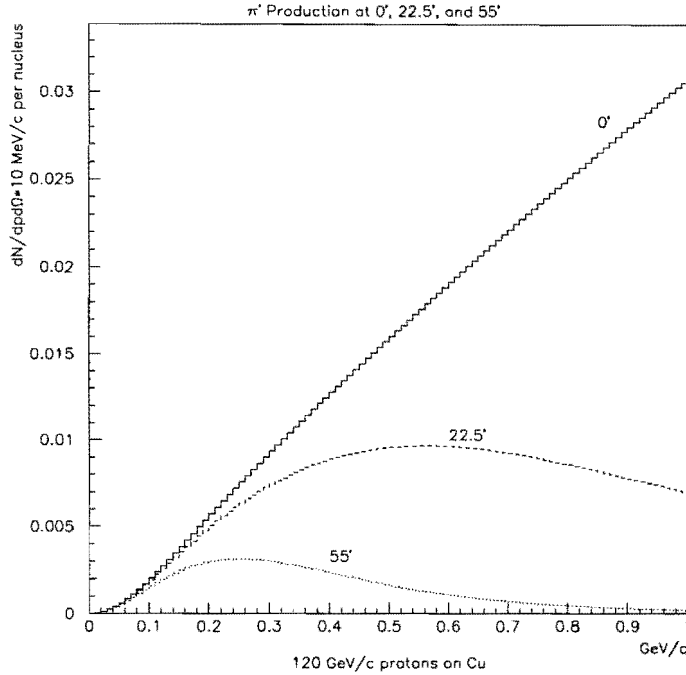


Figure 25: MARS calculation of the π^+ yields at 0° , 22.5° , and 55° for 120 GeV/c protons incident on a copper target.

backgrounds for the cooling channel test measurements.

5.2.1 Fermilab Main Injector Beam Scenario

Our initial calculations indicate that, with a 120 GeV/c primary proton beam incident on the pion production target, at the exit of the muon channel there will be 8.9×10^{-9} muons per incident proton that are within the momentum acceptance and transverse phase-space acceptance of the cooling apparatus. The calculated beam properties are shown in Fig. 26. Matching this beam into the cooling setup is under study.

The Main Injector beam has a 19 ns long micro-structure consisting of a 3 ns period with beam and a 16 ns period with no beam. If there are N_p protons on target per spill of length T_{spill} secs, the rate of muons through the instrumentation during the spill will be given by:

$$R_0 = \frac{N_p}{T_{spill}} \times (8.9 \times 10^{-9}) \text{ Hz} \quad (4)$$

where R_0 is averaged over a timescale much longer than 19 ns. Choosing $N_p = 5 \times 10^{12}$ protons per spill and $T_{spill} = 1$ sec yields a rate $R_0 = 44$ kHz, giving about 0.3 muons in

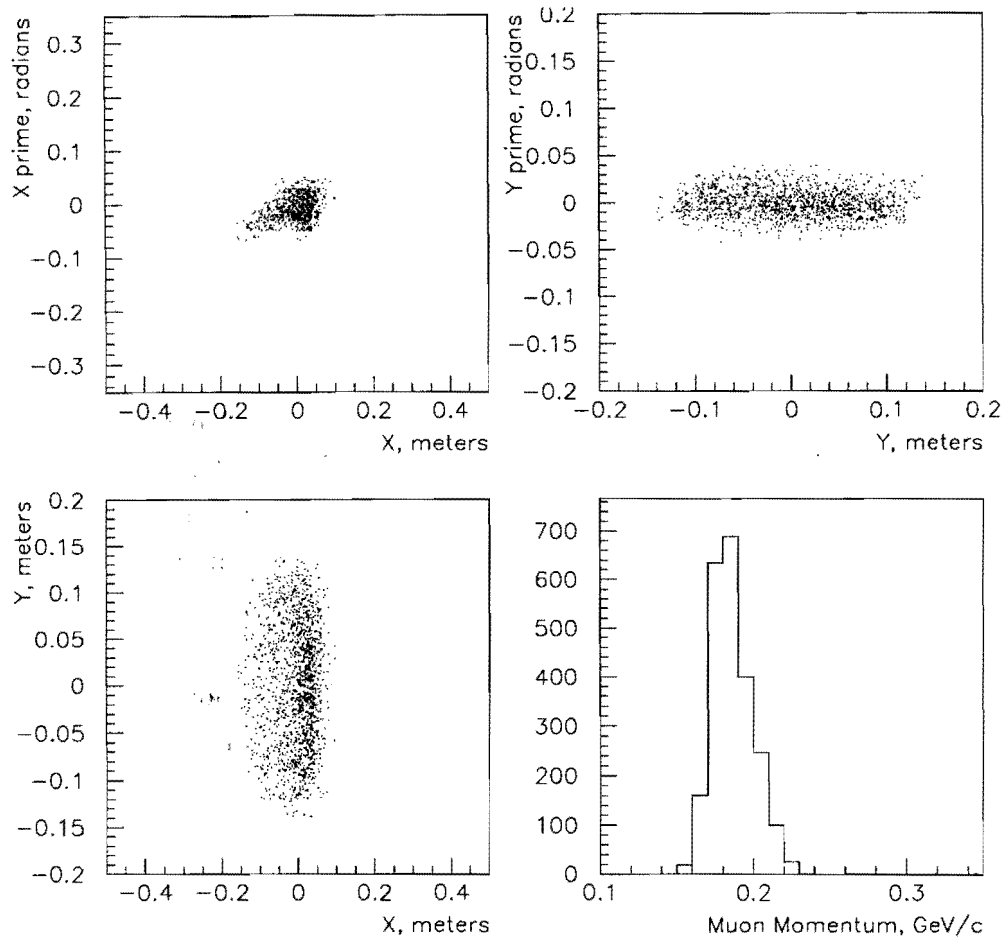


Figure 26: Calculated properties of the 187 MeV/c muon beam at the end of the low energy muon beamline described in the text. The calculation was performed for 120 GeV/c primary protons incident on a 1.5 interaction length copper target. The momentum spectrum (bottom right) is shown before a dp/p requirement of $\pm 5\%$ is imposed to obtain the rates described in the text.

a $6 \mu\text{s}$ interval. Hence the instantaneous data taking rate does not appear to be an issue.

We next estimate the average rate of recording useful data. If the Main Injector is cycling with a period T_{cycle} , the average rate of muons passing through the experiment within the momentum and transverse acceptance of the cooling channel is given by:

$$R_{av} = R_0 \times \frac{T_{spill}}{T_{cycle}}, \quad (5)$$

which, for $R_0 = 44 \text{ kHz}$, and $T_{cycle} = 3 \text{ secs}$ yields $R_{av} = 15 \text{ kHz}$. The cooling channel re-acceleration RF will be pulsed at about 15 Hz , with each RF pulse of $33 \mu\text{s}$ duration. Hence the fraction of the proton spill time in coincidence with the live-time of the RF system is $\sim 5 \times 10^{-4}$. Only 5% of the muons arriving during the RF live-time are also within the useful part of the RF acceleration cycle. These factors introduce an RF efficiency factor of $f_{RF} \sim 2.5 \times 10^{-5}$. Hence the rate of usable muons would be about 0.4 Hz with 5×10^{12} protons on target per spill. With this “event” rate we could make about one measurement per shift with $\sim 10^4$ muons per measurement, or one “high-statistics” measurement per week with $\sim 10^5$ muons.

We note that although 5×10^{12} protons on target within a continuous 1 sec spill from the Main Injector would provide sufficient muons for our measurements, there may be a more optimal primary beam time structure that would reduce the total number of protons we require on target. For example, we are considering the possibility of extracting the beam in 2 msec long “pings”, with 15 pings per Main Injector cycle being delivered to the Meson Hall. Approximately 10^{11} protons per ping would saturate the instantaneous data rate, and provide a more efficient use of the Main Injector protons. More study is required to understand the feasibility of transporting to the Meson area a beam with this more optimal time structure, whilst operating a slow spill program for the KAMI experiments.

5.2.2 Fermilab Booster Beam Scenario

Our calculations indicate that, with an $8 \text{ GeV}/c$ primary proton beam incident on a thin (2% absorption) production target, at the exit of the muon channel there will be 7.9×10^{-12} muons per incident proton that are within the momentum acceptance and transverse phase-space acceptance of the cooling apparatus. The yield can be made larger with a thicker target. However the maximum desirable yield is limited by the maximum tolerable instantaneous rate within the instrumentation, and a low yield is therefore desirable.

The Booster provides up to 5×10^{12} protons per batch cycling at 15 Hz. A Booster batch is 2.1 μsec in duration. If 1×10^{11} protons are extracted per batch then within the 2.1 μsec pulse there will be on average 0.8 muons within the momentum and transverse acceptance of the cooling apparatus, of which 5% will also be within the RF acceptance of the cooling channel. Hence, if one third of the Booster cycles were available for the experiment (5 Hz repetition rate), the average rate of useful muons traversing the cooling test channel would be 0.2 Hz. With this “event” rate we could make about one measurement per day, with $\sim 10^4$ muons per measurement, or one “high statistics” measurement in ~ 1 week with $\sim 10^5$ muons per measurement.

5.3 Measurement Requirements

To study the performance of the prototype alternating solenoid, wedge, and lithium lens cooling components described previously we propose to measure the trajectories of individual muons before and after the cooling apparatus with the cooling setup installed in a muon beam with the appropriate central momentum. This will enable us to select a subset of incoming muons corresponding to an ideal input bunch. The measurements of the incoming and outgoing muons that need to be made are their directions (x', y') , transverse positions (x, y) , momenta (P) , and arrival time with respect to the RF re-acceleration cycle (t) . These measurements will enable the phase-space volume occupied by the selected population of muons to be determined upstream and downstream of the cooling apparatus, and correlations between the individual initial and final phase-space coordinates to be studied.

In the following we will define the phase-space volume V occupied by the population of selected muons:

$$V = \prod_{i=1}^6 \sigma_i, \quad (6)$$

where σ_i is the rms width of the population of muons along the phase-space coordinate i , and the index i runs over the 6 phase-space variables. The uncertainty on V is given by:

$$\frac{\delta V}{V} = \sqrt{\sum_{i=1}^6 \left(\frac{\delta \sigma_i}{\sigma_i} \right)^2}. \quad (7)$$

If the relative uncertainty is the same in all six variables i , then:

$$\frac{\delta_V}{V} = \sqrt{6} \frac{\delta_{\sigma_i}}{\sigma_i}. \quad (8)$$

We would like to demonstrate the cooling performance of a relatively short (10 m long) cooling section. This short section is expected to reduce V by about a factor of 0.7. To provide an adequate measurement of the cooling, and begin to explore the correlations between the incoming and outgoing muon parameters, we must measure V with a precision of a few %. Therefore, we need to measure the individual σ_i with precisions of 1 – 2%. If the selected sample consists of N muons, then it can be shown that [29]:

$$\left(\frac{\delta_{\sigma_i}}{\sigma_i} \right)^2 = \frac{1}{2N} \left(1 + \frac{\sigma_{D_i}^2}{\sigma_i^2} \right)^2 + \left(\frac{\sigma_{D_i}}{\sigma_i} \right)^4 \left(\frac{\delta_{\sigma_{D_i}}}{\sigma_{D_i}} \right)^2, \quad (9)$$

where $\delta_{\sigma_{D_i}}$ is the systematic uncertainty on the detector resolution σ_{D_i} . In practice we will require $\delta_{\sigma_{D_i}} < \sigma_{D_i}$, for example $\delta_{\sigma_{D_i}}/\sigma_{D_i} < 0.2$ would be a reasonable goal. To explore correlations between the positions in phase-space of the incoming and outgoing muons, we also want the detector resolution to be smaller than the width of the corresponding muon distribution, e.g. $\sigma_{D_i} < 0.2\sigma_i$. If N is large, the first term in the preceding equation can be neglected, and the conditions on $\delta_{\sigma_{D_i}}$ and σ_{D_i} that we have just discussed will yield the desired precision $\delta_{\sigma_i}/\sigma_i \sim 1\%$. If N is small, then the first term in the preceding equation dominates, and $\delta_{\sigma_i}/\sigma_i \sim 1/\sqrt{2N}$. A sample of 10,000 muons would be sufficient to ensure that N is large enough to achieve an overall $\sim 1 - 2\%$ measurement of σ_i .

The precision needed for the timing measurement is $\sigma_{D_t} = 8$ ps. This is very demanding. In practice the time measurement is made at a position displaced from the cooling apparatus. Hence, to extract the arrival time of the muon at the cooling apparatus we must calculate the time-of-flight between the time measuring system and the cooling set-up. The uncertainty on the time of flight, $t = L/\beta_z c = L/\beta c \cos \theta$, due to the uncertainty on the momentum is:

$$\delta t = \frac{L}{\beta^2 c \cos \theta} \delta \beta = \frac{L}{\gamma^2 \beta_z c} \frac{\delta P}{P} \approx 1000 \text{ [ps]} \left[\frac{L}{1 \text{ m}} \right] \frac{\delta P}{P}, \quad (10)$$

where θ is the angle of the trajectory with respect to the z -axis. The extrapolation length in the detector arrangement we are currently considering is 4 m. Hence the desired precision on the time measurement $\delta t < 8$ ps sets a requirement on momentum resolution

Table 7: Measurement precisions required to obtain a few % measurement of the phase space volume occupied by the populations of incoming and outgoing muons for the alternating solenoid cooling test.

Variable	Expected	Required	Required
i	input σ_i	σ_{D_i}	$\delta_{\sigma_{D_i}}$
x	24 mm	200 μm	$\pm 40 \mu\text{m}$
y	24 mm	200 μm	$\pm 40 \mu\text{m}$
x'	33 mr	5 mr	$\pm 1 \text{ mr}$
y'	33 mr	5 mr	$\pm 1 \text{ mr}$
P	5 MeV/c	0.23 MeV/c	$\pm 0.05 \text{ MeV/c}$
t	40 ps	8 ps	$\pm 2 \text{ ps}$

$\sigma_{D_P}/P < 0.002$. To allow for other contributions to the uncertainty on the time measurement we will want to achieve a momentum resolution a factor of $\sqrt{2}$ better than this, and we arrive at the final momentum resolution requirement $\sigma_{D_P}/P < 0.0014$. A careful consideration of the precisions required for all six phase-space variables leads to the results summarized in Table 7.

5.4 Detector Design

We are currently designing a detector scheme that can measure the 6 phase-space variables for the incoming and outgoing muons with the desired precisions. The scheme we are investigating is shown in Fig. 27, and consists of an upstream measuring system, the cooling apparatus to be tested, and a downstream measuring system that is a mirror image of the upstream system. The upstream measuring system is shown in more detail in Fig. 28. To contain the large transverse emittances of the incoming muon populations, the upstream detectors are inside a solenoidal field coaxial with the beam direction. The instrumentation within the solenoidal channel consists of (i) an initial (auxiliary) time measurement device to locate the particles within $\sim 1/4$ RF cycle, (ii) the first time projection chamber (TPC 1) to measure the particles trajectory preceding the first bend in the solenoid channel, (iii) TPC 2 following the first bent solenoid and hence determining the initial particle momentum, (iv) an RF acceleration cavity phase locked to the ioniza-

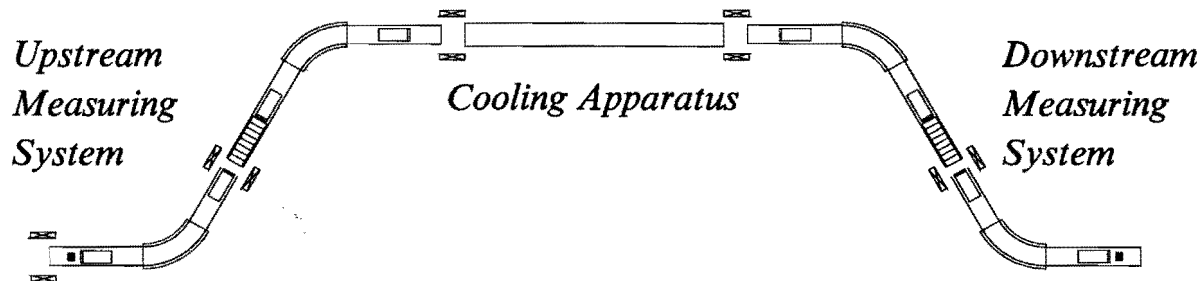


Figure 27: Schematic of a detector arrangement to measure the 6 phase-space variables for the incoming and outgoing muons with the precision discussed in the text.

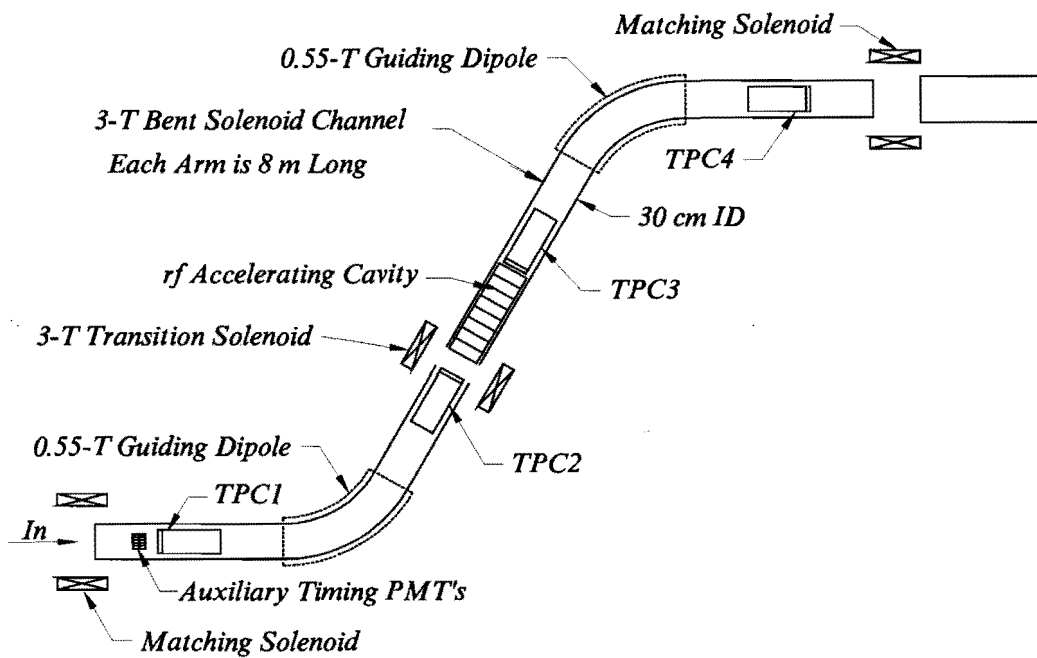


Figure 28: Schematic of upstream measuring system.

tion cooling RF re-acceleration cavities, (v) TPC 3 following the RF cavity and preceding the second bent solenoid, (vi) TPC 4 following the second bent solenoid and hence determining the momentum after the accelerating cavity and the trajectory of the particle incident on the cooling apparatus. The detector components are discussed in more detail in the following subsections.

5.4.1 Time Measurement

The demanding timing requirement has a strong influence on the overall choice of measuring techniques. The precision needed for the time measurement cannot be achieved by a conventional particle detector. We have investigated using an RF cavity to provide a time-dependent transverse- or a time-dependent longitudinal-kick to the traversing muons, and then extracting the arrival time by measuring the size of the kick. At present we believe the best option is the use of an RF accelerating cavity phased to impart zero energy to a particle in time with the re-acceleration RF cycle. This will result in a correlation between the energy (and hence momentum) given to the muon in traversing the cavity and its arrival time. If we use an 11 cell acceleration cavity of the same design used in the alternating solenoid cooling section, and operated in the $TM_{0,1,0}$ mode with a peak field of 30 MV/m, then the cavity will change the particles energy by:

$$\Delta U = 0.16 \text{ [MeV]} \left[\frac{\Delta t}{1 \text{ ps}} \right], \quad (11)$$

which will result in a momentum change:

$$\frac{\Delta P}{P} = 0.001 \left[\frac{\Delta t}{1 \text{ ps}} \right]. \quad (12)$$

Measurement of the muon's momentum before and after the RF cavity permits inference of the desired time. This technique requires a fourfold momentum measurement of each muon: twice before the cooling apparatus and twice after. We require a momentum resolution $\sigma_{D_p}/P = 0.008/\sqrt{2}$ to achieve a time resolution $\sigma_{D_t} = 8$ ps. This is less stringent than the requirement on the momentum measurement arising from the precision with which the time must be extrapolated to the cooling setup (discussed previously).

In addition to the main time measurement, an auxiliary measurement with a precision of about 300 ps or better is required to determine the correct quarter-period of the RF

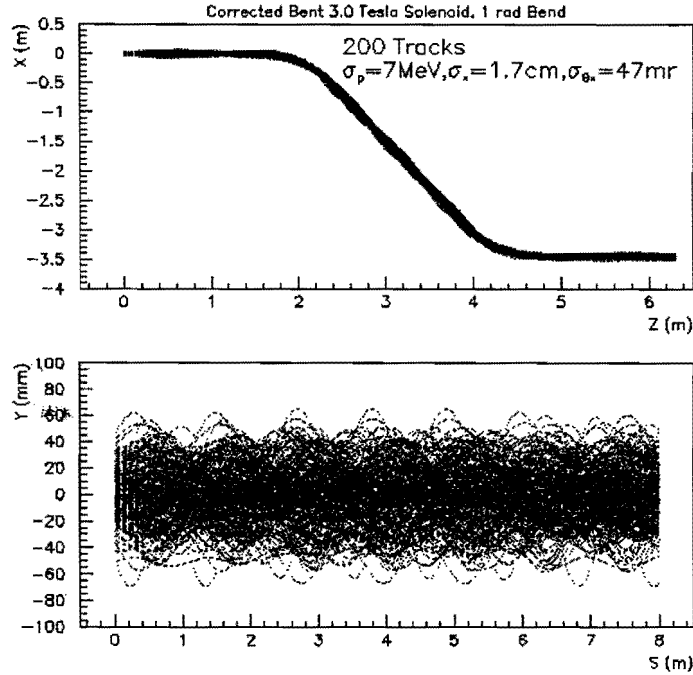


Figure 29: Orbits of 200 muons chosen at random from within the Gaussian phase-space volume specified in Table 8, projected onto the horizontal and vertical planes.

cycle. This auxiliary measurement would also provide the T_0 for the experiment, and combined with the main timing measurement, would provide time-of-flight information over a ~ 3 m flight path that could be used to reject incoming pions and electrons. The time-of-flight difference per meter between particles of masses m_1 and m_2 at momentum P is given by:

$$\Delta t = \frac{1}{\beta_1 c} - \frac{1}{\beta_2 c} = \frac{\sqrt{1 + (m_1 c/P)^2} - \sqrt{1 + (m_2 c/P)^2}}{c}. \quad (13)$$

At 187-MeV/ c , electrons arrive earlier than muons by 0.5 ns/m and pions arrive later by 0.34 ns/m. The time-of-flight measurement would benefit from a more precise auxiliary timing measurement than 300 ps. The auxiliary timing measurement is therefore described in more detail in section 5.4.4.

Table 8: Parameters of the 1.5 T and 3 T bent-solenoid channels that have been studied for the upstream and downstream measuring systems with a central beam momentum of 165 MeV/c.

Parameter	Value	Value
F_{RF}	800 MHz	400 MHz
P_{muon}	165 MeV/c	165 MeV/c
B_{Guide}	0.55 T	0.55 T
B_s	3 T	1.5 T
θ_{bend}	1 rad	1 rad
R_{bend}	1 m	1 m
λ_{cycl}	1.15 m	2.30 m
R_s	15 cm	24 cm
L_s	4 m	4 m
β^*	36.7 cm	73.3 cm
$\sigma_x = \sigma_y$	17 mm	24 mm
$\sigma_{x'} = \sigma_{y'}$	47 mrad	33 mrad
L_{tracking}	43 cm	57 cm
n	33 clusters/m	33 clusters/m

5.4.2 Solenoidal Channel

An elegant way of providing the dispersion required for the momentum measurement is to exploit the confining solenoidal field by using ‘bent solenoids’. In Fig. 27 a total of four bent solenoids are linked by straight solenoids to form the muon channel of the detector. If the bending plane of the bent solenoids is horizontal, the beam experiences a net vertical displacement (called ‘curvature drift’ in the plasma-physics community) of $O(10 \text{ cm})$. In the proposed detector configuration, the curvature drift is canceled for muons having the central beam momentum. This is accomplished by using ‘guiding dipole’ magnets to provide an additional vertical field $B_G = 0.55 \text{ T}$ superimposed on the field provided by

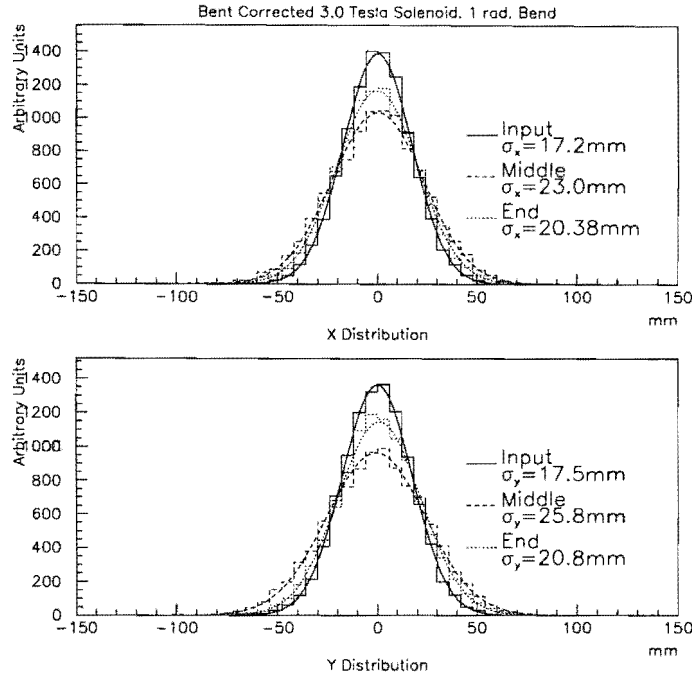


Figure 30: The distribution of muons along horizontal and vertical axes at the beginning, middle (= RF timing cavity) and end of the upstream bent solenoid channel.

the bent solenoid. Off-momentum muons are displaced vertically by an amount:

$$\Delta y \approx \frac{P}{eB_s} \frac{\Delta P}{P} \theta_{\text{bend}}, \quad (14)$$

where B_s is the field of the bent solenoid and θ_{bend} is the bend angle. Note that eq. (14) describes the deflection of the ‘guiding ray’ (or axis) of the helical muon trajectory and not the trajectory itself. The muon’s momentum cannot be determined simply by measuring the height of its trajectory at the entrance and exit of a bent solenoid. Rather, the height of the guiding ray must be reconstructed at both places, which requires precise measurements of the helical trajectories. The momentum resolution of a bent solenoid spectrometer is given by:

$$\frac{\sigma_{DP}}{P} \approx \frac{1}{\theta_{\text{bend}}} \frac{P}{eB_s} \frac{\sigma_{D_x}}{L^{5/2}} \sqrt{\frac{720}{n}}, \quad (15)$$

where L is the length of the trajectory observed (before and after the bend) with n samples/m, each with transverse spatial resolution σ_{D_x} . As expected, the momentum resolution improves with increasing magnetic field. However, to lower the cost of the

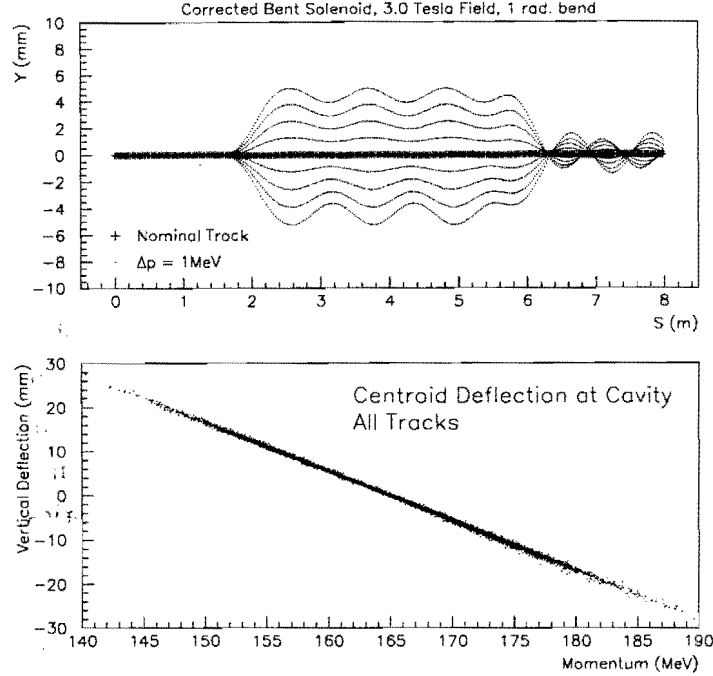


Figure 31: (a) Vertical projection of trajectories of muons that initially lie along the central ray, but depart from the central momentum by 1 MeV/c increments. The vertical momentum dispersion between the bent solenoids is evident. (b) Summary of vertical deflection of the guiding ray of muons as a function of their momentum. Compare to eq. (14).

solenoid channel we will want to use a relatively low magnetic field. The momentum resolution is improved by increasing θ_{bend} and by increasing L . Since it would be difficult to assemble a planar transport system with $\theta_{\text{bend}} > \pi$, we will choose $\theta_{\text{bend}} \sim 1$ radian. We require that the solenoid channel transmit 99.9% of the beam, and therefore its inner radius must be 3.3 times the largest rms transverse width of the beam in the channel.

In our initial studies we have considered a muon beam with a central momentum of 165 MeV/c propagating through (a) a 3 T solenoidal channel with an inner radius of 15 cm, and (b) a 1.5 T solenoidal channel with an inner radius of 24 cm. The parameters for these two choices are listed in Table 8. Further studies are in progress to understand the optimum choice of solenoid parameters and their dependence on the beam momentum. In the following we describe the higher field ($B_s = 3$ T) case.

We have performed a numerical simulation of the muon trajectories within the 3 T solenoidal channel by integrating the equations of motion. At present we assume that the

horizontal fields within the straight solenoid sections are those of an ideal solenoid, and those in the bent solenoids are those of an ideal toroidal sector. Likewise, ideal vertical guiding fields are superimposed on the bent solenoids. Thus Maxwell's equations are piecewise satisfied, but suffer discontinuities at the boundaries between straight and bent solenoids. Figure 29 shows the orbits of 200 muons selected at random from within the Gaussian phase-space volume specified in Table 8. The periodicity of the orbits with λ_{cycl} is readily evident in the upstream part of the channel, but is washed out due to chromatic effects by the end of the channel. Figure 30 shows the x and y profiles of the beam at the beginning, middle, and end of the channel. The profiles broaden after the first bend due to the momentum dispersion. Figure 31(a) shows the trajectories of muons that lie along the central ray upstream of the first bend, but differ from the central momentum in increments of 1 MeV/ c . The vertical dispersion caused by the bent solenoid is evident. Figure 31(b) shows the vertical displacement of the guiding ray of 200 random muons as a function of their momentum, in agreement with eq. (14).

5.4.3 Low-Pressure Time-Projection Chambers

The momentum measurements require precise measurements of the helical muon trajectories in the solenoidal fields before and after the bends. Since the muons have relatively low momentum, multiple scattering in detector material, and even in atmospheric-pressure gas, will significantly degrade the momentum resolution. Hence, we propose that each arm of the momentum measuring system be a low-pressure device with minimal internal structure.

As an example, we are considering using 8.4-Torr methane at 20°C as the ionization medium in an ionization chamber, yielding one ion pair per 3 cm of track length. Equation (15), with $n = 33$ clusters/m, leads to the choice $L = 43$ cm for the length of the tracking devices. In the strong magnetic field of the detector the ionization electrons drift easily only along the field lines. Hence the drift electric field should be aligned with the magnetic field, leading to a time-projection chamber (TPC) geometry. The drift velocity of ionization electrons is a function of E/P , where E is the electric field and P is the gas pressure. The saturation drift velocity of 100 $\mu\text{m}/\text{ns}$ (methane) is achieved at a field of only 10 V/cm at 8.4-Torr pressure. The proposed TPC is not a high-voltage device. Gas gain is obtained near a wire mesh anode plane in a gap separated from the ionization/drift

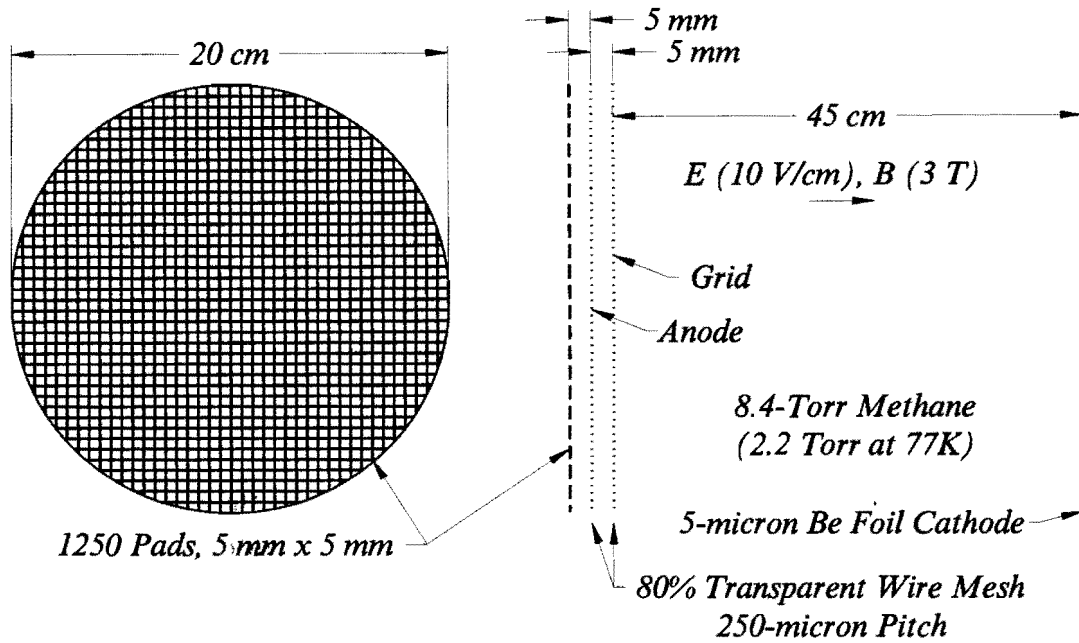


Figure 32: Sketch of the low-pressure time projection chamber.

region by a wire-mesh grid, as shown in Fig. 32. The induced pulse on a cathode plane subdivided into 1250 $5 \times 5 \text{ mm}^2$ pads yields x and y coordinates to $200 \mu\text{m}$ via charge interpolation. Each pad is sampled at 50 MHz, and the samples are stored in a 512-deep switched-capacitor array and multiplexed into a 12-bit ADC between beam pulses. Interpolation of the samples in time will locate the z coordinate to $200 \mu\text{m}$. Over a total drift distance of 45 cm, the TPC will observe 15 points on a track segment, and measure its angle with a precision of about 1 mrad. The momentum resolution of each TPC-bent solenoid-TPC spectrometer will be $\sigma_P/P = 0.0014$ at 165 MeV/c.

The total drift time of the ionization electrons is about $4.5 \mu\text{sec}$, which is of the same order as, perhaps even longer than, the active time of the RF system of the cooling apparatus. So in effect, the detector concurrently samples all muons in a single RF macropulse. To successfully isolate each of these muons there should be no more than about 10 muons per macropulse independent of the pulse length, provided it is in the range $50 \text{ ns} - 6 \mu\text{s}$. A higher rate capability could only be achieved with a detector with shorter drift times, and hence more walls and higher channel count. The additional walls will compromise the angular resolution due to multiple scattering, while the higher channel count raises the detector cost.

Table 9: Time-of-flight differences for $\mu - e$ and $\pi - \mu$ separation over a 3 m flight path, shown as a function of particle momentum.

p	MeV/c	25	50	100	187	200	260	300
$\mu - e$	ns	33.2	13.4	4.54	1.48	1.31	0.80	0.60
$\pi - \mu$	ns	13.3	6.27	2.63	0.99	0.89	0.56	0.43

5.4.4 Particle Identification

To ensure that the particles used to measure the performance of the cooling apparatus are muons, we will need to identify incoming pions at the upstream end of the upstream measuring system. We will also need to identify and reject electrons from muon decays at the downstream ends of the upstream and downstream measuring systems. A combination of time-of-flight and threshold cherenkov measurements can accomplish this.

Table 9 summarizes $\mu - e$ and $\pi - \mu$ time-of-flight differences over a 3 m flight path as a function of particle momentum. A 300 ps auxiliary time measurement approximately 3 m from the main (RF cavity) time measurement, would provide $\mu - e$ separation at better than ~ 2 standard deviations over the entire momentum range of interest, and $\pi - \mu$ separation at better than ~ 1.5 standard deviations. We would benefit from a more precise auxiliary time measurement. A 150 ps time measurement would ensure a $\pi - \mu$ time difference of better than ~ 3 standard deviations, which should be adequate since the calculated pion contamination in the muon beam is small ($< 1\%$).

To achieve good time resolution, we propose to make the auxiliary time measurements using 2 mm diameter scintillating fibers read out with photomultiplier tubes. The scintillating fibers will be organized into ribbons with each end of each scintillating fiber spliced to a clear fiber. The clear fibers take the light to photomultiplier tubes that are located outside of the high magnetic field region. The lengths of the scintillating fibers are then chosen to form an active area with the appropriate shape and size (Fig. 33). To ensure sufficient light from the passage of a muon through the fiber array, each auxiliary timing counter will consist of about 15 fiber layers. We expect 10 to 15 photoelectrons per MIP (minimum ionizing particle) to be collected from each fiber end [18]. If we use one-inch Hamamatsu R5322 PMTs, which have a time transfer spread of 160 ps (full width half max), we will require forty-eight tubes to build two auxiliary timing arrays, one for the

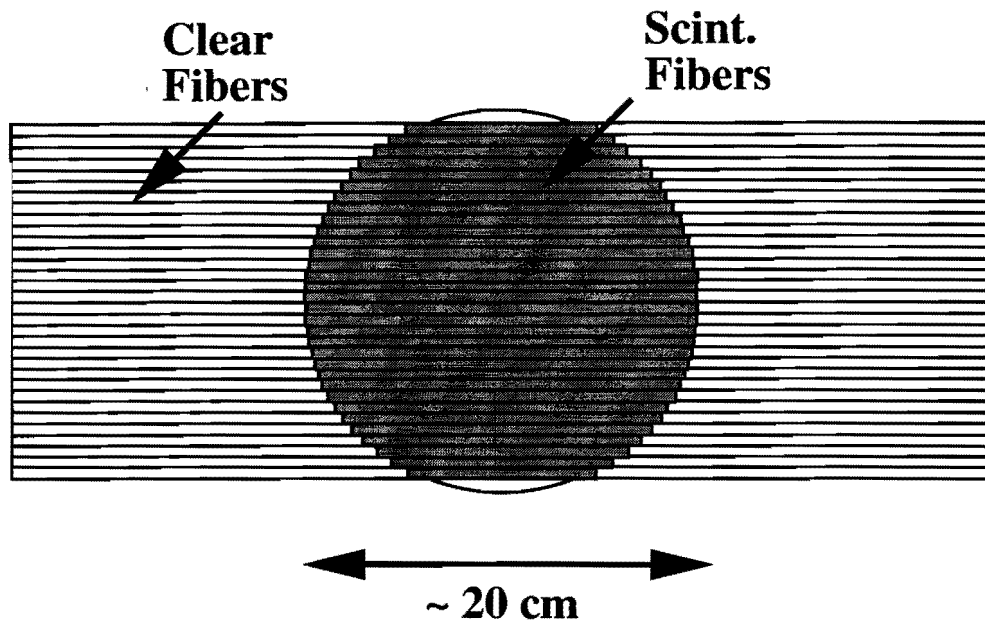


Figure 33: Scintillating fiber arrangement for the auxiliary time measurement device.

upstream arm and one for the downstream arm. The readout will require discriminators, TDCs, and ADCs. One hundred picosecond timing measurements should be possible with this Auxiliary Timing System.

A significant fraction of the incoming muons will decay whilst traversing the instrumentation channels, and it will therefore be necessary to supplement the time-of-flight system with additional electron rejection systems at the downstream ends of both the upstream and downstream instrumentation arms. We propose to use threshold cherenkov counters to provide compact electron taggers at the desired locations. A range of suitable cherenkov media exist that cover the momentum range of interest (Table 10). Silica aerogel can be used to discriminate between muons and electrons over a 100 to 300 MeV/c momentum range. A 12 cm thick 0.10 g/cm^3 silica aerogel counter would provide about 40 photoelectrons per MIP.

Finally, since incoming pions that decay as they traverse the upstream measuring arm

Table 10: Cherenkov thresholds for electrons, muons, and pions. The refractive indices for C_6F_{14} and C_2F_6 are for 350 nm and are approximations based on linear extrapolations (T. Ypsilantis and J. Seguinot, NIM A343 (1994) 30).

Material	Density g/cm ³	X_0 mm	Length mm/15pe	Refractive Index(n)	Electron MeV/c	Muon MeV/c	Pion MeV/c
Polystyrene	1.03	424	4	1.581	0.42	86	114
Quartz	2.20	123	4	1.458	0.48	99	132
Water	1.00	361	5	1.33	0.58	120	159
C_6F_{14}	1.68	206	6	1.244	0.69	143	189
C_2F_6	1.61	~200	7	1.222	0.73	150	199
LN_2	0.81	471	7	1.205	0.76	157	208
LD_2	0.18	7540	10	1.128	0.98	202	267
LH_2	0.071	8900	12	1.112	1.05	217	287
LN_e	1.206	240	14	1.092	1.16	241	318
Aerogel	0.30	995	16	1.075	1.30	268	354
Aerogel	0.20	1490	24	1.050	1.60	330	436
Aerogel	0.15	1990	31	1.038	1.84	379	501
Aerogel	0.10	2985	46	1.025	2.27	470	620

can also confuse the time-of-flight particle ID measurement, we are also considering using a threshold cherenkov counter for pion tagging at the upstream end of the upstream measuring system. For example, a 187 MeV/c muon passing through a 2 cm thick slab of C_6F_{14} from the 3M Company in Minneapolis would yield ~ 40 photoelectrons. This material should therefore work well as a cherenkov counter to discriminate between 187 MeV/c pions and muons. Liquid hydrogen or dense silica aerogel are candidates for separating 260 MeV/c muons from pions. Note that dense 0.40 g/cm³ silica aerogel may require some development.

5.4.5 Trigger and Data Acquisition

The trigger for the cooling test experiment would be based on a coincidence between the auxillary time measurement scintillators and particle ID detectors within the livetime of the re-acceleration RF. If we make no attempt to also require the particles to arrive within the useful $\sim 5\%$ part of the RF cycle, we will record data at up to about 10 Hz, with total

data samples of a few $\times 10^5$ - 10^6 “events” per measurement, and measurements taking typically from one day to one or two weeks.

The total number of readout channels will be modest. We anticipate eight TPCs, each with 1250 pads, 48 PMTs for the auxillary time measurement, and a small number of PMTs (or equivalent) for additional particle identification devices. In addition we will want to add accelerator status information to the event record. Although a full design of the data acquisition system has still to be done, we believe that our DAQ needs are relatively modest. We anticipate using readout modules that already exist at the laboratory, and commodity computers for the online system.

5.5 Simulation of the Experiment

We are developing two simulation tools to facilitate a detailed simulation of the muon beamline, instrumentation channel, and cooling apparatus. The first tool[19] (ICOOL) is a “fast” 3-dimensional tracking program that is specifically being developed to study ionization cooling. The second code[21] (DPGEANT) is an extended version of the well known GEANT program.

5.5.1 ICOOL

The ICOOL program simulates particle-by-particle propagation through materials and electromagnetic fields, including solenoids, dipoles, and time varying fields (RF cavities). Physics processes relevant to the propagation and interaction of low energy (sub-GeV) muons are simulated, namely decays, multiple scattering, and energy loss. The code for Moliere scattering and for straggling using the Landau and Vavilov distributions was adapted from GEANT v3.21 with minimal interface changes. Incident beam particles can be generated from uniform or Gaussian distributions, or read from an input file. The individual particles are tracked through regions which are described using “accelerator” coordinates. Every region has associated with it a specified material and field type, and ICOOL uses analytic models to compute field strengths at each location. For each tracking step the program updates the particle position and momentum, taking into account the local field, and correcting the particle’s momentum for energy loss and multiple scattering.

ICOOL has been used to study the cooling capability of the cooling section that we are proposing to build and test. In Table 11 the calculated beam parameters after the

Table 11: ICOOL predictions for the beam parameters at the downstream end of the 10 m transverse cooling section we are proposing to build, compared with the corresponding parameters at the input of the cooling section. Note: The P_z and t distributions are not Gaussian.

Location		0 m	10 m
P_{ref}	MeV/c	187	187
Losses	%	0	0.6
σ_x	mm	7.91	6.98
σ_y	mm	8.01	6.96
σ_t	ps	43.4	53.9
σ_{Px}	MeV/c	25.2	20.4
σ_{Py}	MeV/c	24.8	20.7
σ_{Pz}	MeV/c	6.04	8.26
ϵ_{TN}	mm mr	1305	897
ϵ_{LN}	mm	0.649	1.045
ϵ_{6N}	$\times 10^{-12} m^3$	1105	841

10 m cooling test section are compared with the corresponding parameters at the input of the cooling section. The ICOOL calculations predict that the test cooling channel will reduce the transverse normalized emittance by a factor of 0.69, and the 6-dimensional normalized emittance by a factor of 0.76. The longitudinal normalized emittance grows in this section, as expected, by a factor of 1.61.

To study the effects of the finite detector resolutions listed in Table 7 we have smeared the input and output positions of the simulated muons in 6-dimensional phase-space by the appropriate Gaussian resolution functions ($\sigma_x = \sigma_y = 0.2$ mm, $\sigma_t = 8$ ps, $\sigma_{Px} = \sigma_{Py} = 0.93$ MeV/c, $\sigma_{Pz} = 0.23$ MeV/c). The resulting predictions for the measured input and output phase-space volumes occupied by the muons are summarized in Table 12. As expected, the measurements are sufficiently precise to determine the performance of the cooling channel to O(1%). The predicted two-dimensional transverse beam profile is shown in Fig. 34 at the upstream and downstream ends of the cooling channel. The simulated measured “beam spot” clearly shrinks as the muons pass through the cooling section. Indeed, the average radial distance from the beam axis and the average muon transverse momentum are both reduced, whilst the longitudinal distributions are slightly

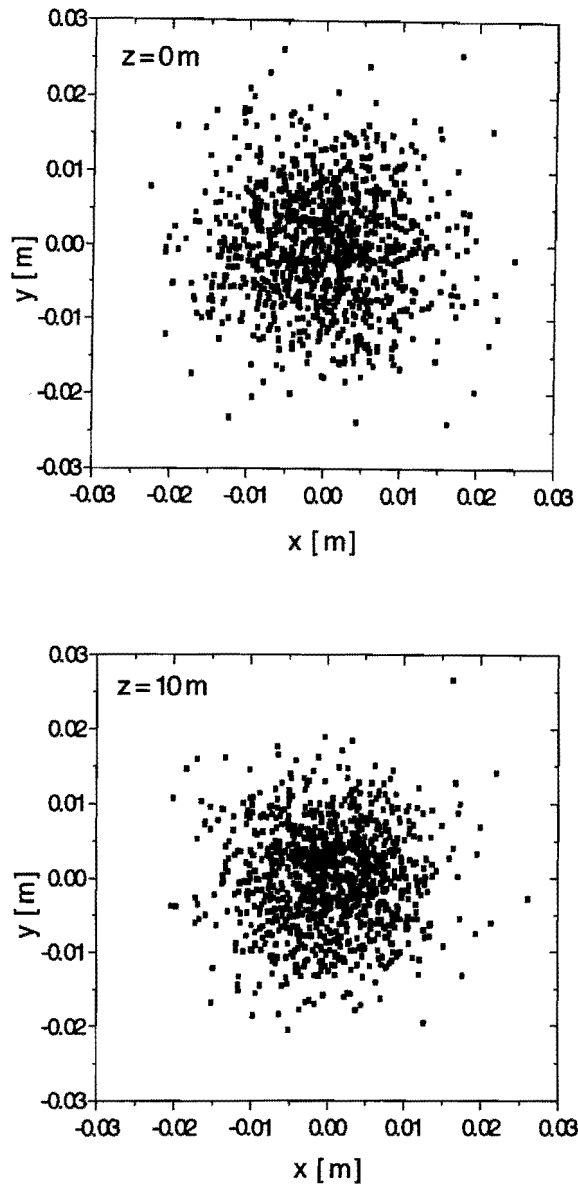


Figure 34: ICOOL predictions for the measured muon populations in the transverse plane at the input (top plot) and output (bottom plot) of the 10 m long transverse cooling test section.

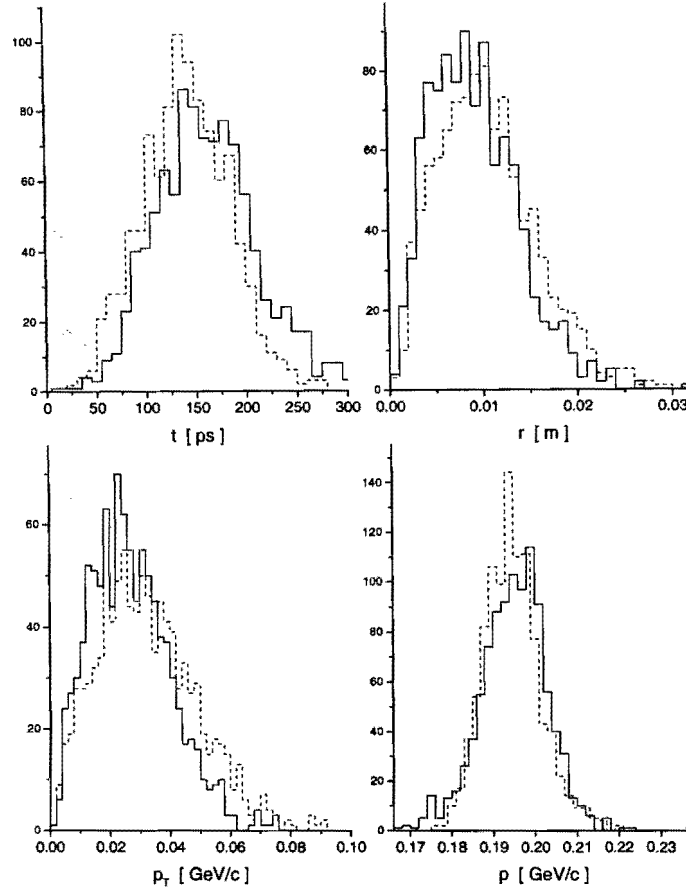


Figure 35: ICOOL predictions for the measured muon populations at the input (broken histograms) and output (solid histograms) of the 10 m long transverse cooling test section. The distributions shown are (a) arrival time with respect to the reference particle (top left), (b) radial position in the transverse plane (top right), (c) transverse momentum with respect to the beam axis (bottom left), and (d) momentum (bottom right).

Table 12: ICOOL predictions for the measured transverse, longitudinal, and 6-dimensional phase-space volumes occupied by the muon beam at the input and output of the test transverse cooling channel. The predictions are based on simulating 1000 muons traversing the cooling channel. The quoted uncertainties are computed by repeating the simulation 10 times.

Location		0 m	10 m
ϵ_{TN}	mm mr	1323 ± 2	900 ± 4
ϵ_{LN}	mm	0.651 ± 0.006	1.059 ± 0.006
ϵ_{6N}	$\times 10^{-12} m^3$	1139 ± 9	858 ± 8

degraded (Fig. 35).

5.5.2 DPGEANT

The GEANT Monte Carlo program is a simulation tool that has been developed over a number of years and is widely used in the particle physics community for detector design and analysis studies. However it has not been developed for accelerator physics applications, and must be enhanced if it is to be of use in simulating the ionization cooling channel test. In particular:

- (i) The precision of the tracking in GEANT is insufficient for accelerator applications in which particles must be precisely followed over path lengths much greater than a few meters. A double precision version of the program (DPGEANT) is required.
- (ii) The program must be able to handle time-varying fields (i.e. RF cavities), and any other components required in the cooling channel and for the cooling facility instrumentation (for example, bent solenoids).
- (iii) The program must have a more precise description of large angle scattering than is currently implemented in the GEANT code.
- (iv) An input/output interface with ICOOL is desirable so that a common set of particles can be tracked using the two programs, and a comparison made.

We are developing DPGEANT to enable a full simulation of the cooling experiment to be performed. Most of the required enhancements to the GEANT code are in place, and

muons traversing the test cooling channel have been simulated (see Fig. 13). Cross-checks of the ICOOL results are in progress and work on a DPGEANT simulation of the low energy muon beamline has started. We anticipate that in a few weeks the program will be ready to begin simulating the entire cooling setup (beamline + instrumentation + test cooling channel).

5.6 Cooling Test Facility: Layout and Location

The cooling test facility must be located so that it can receive a primary proton beam, either a 120 GeV/c Main Injector beam, or an 8 GeV/c Booster beam. Our preliminary beamline studies suggest that either of these beams would be able to provide a suitable source of pions (and hence muons) for the ionization cooling tests. Candidate locations for the test facility are the Fermilab Meson Hall or a new area receiving beam from the Fermilab Booster. Ultimately, the choice of location for the cooling test facility must take into account costs, and laboratory schedules, etc. We believe that it is important that the ionization cooling beam measurements begin early 2002 so that the ionization cooling technique can be fully explored well before the turn-on of the LHC.

Conceptual schematics of an initial layout for the ionization cooling test facility are shown in Figs. 36 and 37, with the facility installed in respectively the MCenter and MWest beam-lines of the Fermilab Meson Hall. Protons from the Main Injector are incident on a target and dump located towards the downstream end of the hall. The low energy muon beamline bends backwards to inject muons into the cooling setup such that the upstream end of the apparatus is at the downstream end of the hall. Although it is not a requirement for the experiment, our initial calculations suggest that the shielding around the cooling setup will be sufficient to allow one hour controlled occupancy with the muon beam on. The shielding at the north end of the apparatus, which faces the location of the proposed Main Injector Kaon experiments, serves to protect people from low energy muons and hadrons, and from X-rays generated by klystrons and RF cavities. Heavy shielding around the primary proton beam protects the klystron and power supply galleries. To minimize the length of the water cooled copper beam dump we plan to use a 1.5 interaction length copper pion production target. The target and beam dump are surrounded by sufficient shielding to permit short occupancy at the outside surface, although detailed design around the beam port remains to be done. Concrete shielding

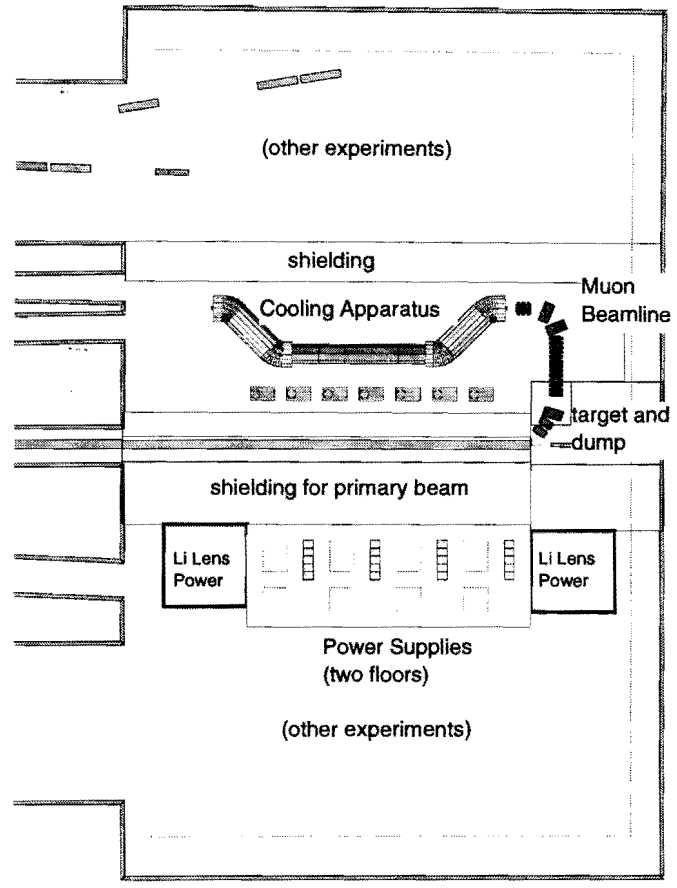


Figure 36: Plan view of a possible cooling facility layout installed in the MCenter beamline of the Fermilab Meson Hall.

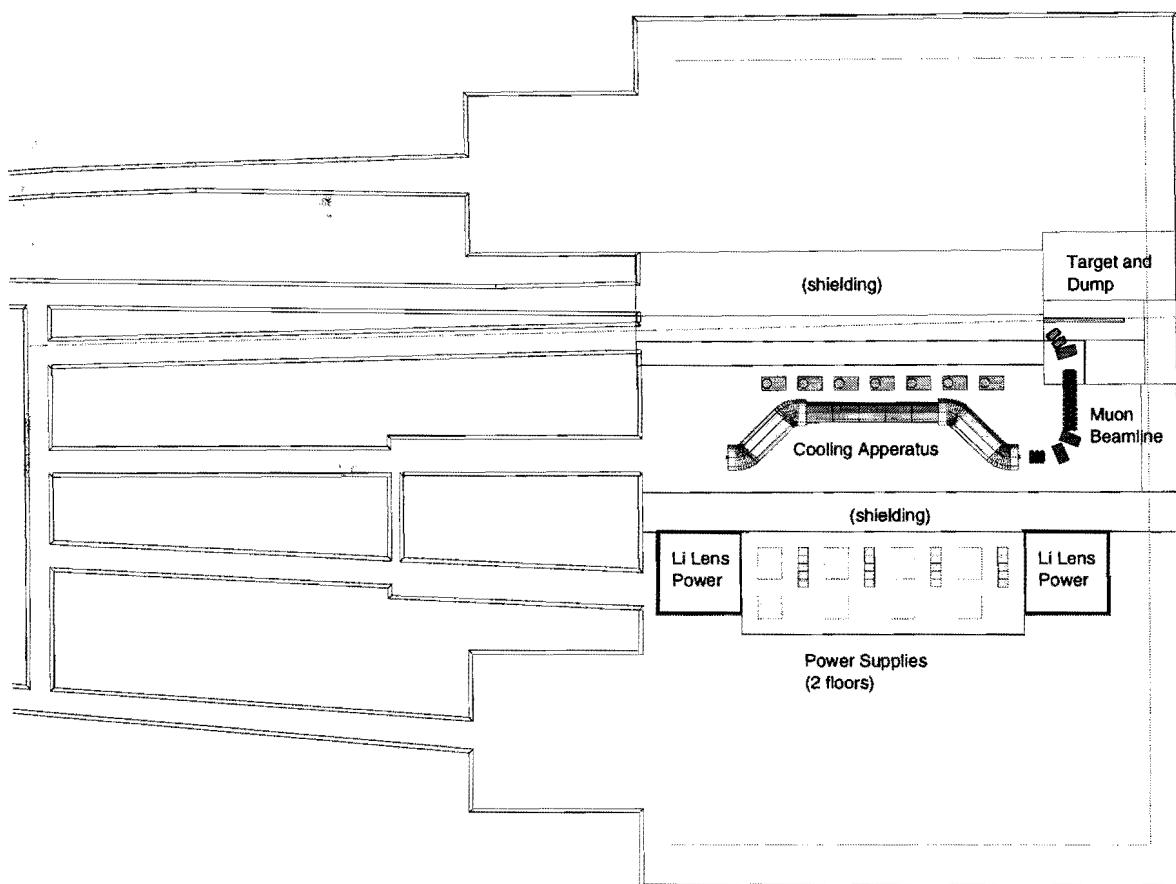


Figure 37: Possible cooling facility layout installed in the MWest beam-line of the Fermilab Meson Hall.

at the back wall of the meson hall contains low energy particles within the building.

The meson detector hall is 40.5 m long, of which 12 m will be needed for the low energy muon beamline, and a further 12 m will be needed for the instrumentation on either ends of the cooling test channel. Hence, the 10 m long alternating solenoid transverse cooling test channel will fit within the hall. A detailed plan will be needed to understand whether the existing hall could also accommodate the other cooling test sections (wedge, and lithium lenses). It will be necessary to either make the cooling apparatus curl up on itself (which may be natural), and/or to extend the meson hall in the neighborhood of the experiment. We note that an advantage of locating an ionization cooling test facility in the Meson Area at Fermilab is that much of the shielding, dumps, and magnets already exist. This area is near a service building that can house power supplies and control electronics. Excellent crane coverage exists in the beamline and beam dump areas. Locating the facility in the Meson Hall may therefore help to enable a timely start to the cooling measurements.

6 R & D Plan: Schedule and Funding

In a few years time the US high energy physics community will need to decide which new accelerator facility or facilities should be proposed and built in the US to provide cutting-edge physics beyond the next decade. If on this timescale a high-luminosity muon collider is to be a candidate for the facility of choice, a vigorous R&D program is essential to develop, test, and optimize the hardware needed to build an ionization cooling channel. In this proposal we have described a program of alternating solenoid, wedge, and lithium lens hardware prototyping and testing that we believe can be accomplished in about six years, and that will enable a complete cooling channel to be confidently designed for the First Muon Collider.

6.1 Schedule

The overall schedule for the R&D program is summarized in Fig. 38. We assume that the program begins now with the low level activities that are already proceeding.

The RF cavity part of the program can be summarized as follows. In the remainder of 1998 we would focus our attention on developing the RF cavities required in the cooling channel. The work would continue through 1999, and include basic material properties

testing of beryllium for the cavity windows, the design, fabrication, and testing of the beryllium windows, construction of a 3-cell cavity for low power tests, design and construction of a 3-cell cavity for high-power tests at liquid nitrogen temperatures in a 5.5 T field, and the preparation of a high power test facility with a 12 MW klystron and a 5.5 T superconducting solenoid to facilitate the high power tests. This part of the R&D program would culminate in a high power test of a 3-cell cavity completed in early 2000.

Assuming the initial RF R&D is successful, the next goal is to construct the first 2 m alternating solenoid transverse cooling section ready for initial beam tests in 2002. The design of the 1.3 m long RF module needed for the 2 m section would be completed early 2000. Fabrication and bench testing of the first RF module would be completed by the end of 2000. The solenoid design would be completed by the end of 1999. Fabrication and assembly of the solenoids for the first 2 m alternating solenoid section would be completed by the end of 2000. The first liquid hydrogen absorber would be designed and constructed in 2000. Instrumentation design and prototyping for the beam tests, and bent solenoid design, would be completed by mid-1999. The goal would be to have all of the upstream and downstream measurement systems constructed and ready for installation by the end of 2000. The measurement systems would then be ready for a calibration run with beam starting mid-2001, prior to installation of the cooling test channel which would begin late in 2001.

The next goal for the alternating solenoid development is the construction of a 10 m cooling section, ready for beam tests in 2003. RF module production for the 10 m section would begin in 2001, and be completed early 2002. Production of the klystrons, power supplies etc would begin late 2000, and be completed late 2002. The solenoids would be fabricated in 2002, and the liquid hydrogen absorber fabrication would begin mid-2002, and be completed early 2003.

In parallel with the alternating solenoid transverse cooling channel development, we propose to also develop a longitudinal (wedge) cooling stage. We anticipate that the wedge cooling prototype design and fabrication would be about 1 year behind the alternating solenoid cooling channel design and initial fabrication. Installation and beam testing of the wedge system would begin at the end of 2002.

The lithium lens part of the R&D program can be summarized as follows. Design work for a 1 m long liquid lithium lens would begin late 1998, and proceed in parallel with the ongoing effort to construct a shorter lens for the Fermilab antiproton program.

The design would be completed late 1999, and fabrication of the first 1 m prototype lens would be completed late 2000. At this time design of a second higher gradient lens would be proceeding, and bench testing of the first lens would begin. The second lens plus power supply would be completed at the end of 2002, and be ready for a lens-RF-lens beam test in 2003.

From 2002 onwards our provisional schedule requires beamtime at the cooling test facility alternating with periods for installation of sections of the cooling channel. Measurements would take place over a two-year period.

6.2 Required Facilities at Fermilab

Our R&D plan requires two facilities at Fermilab:

- (i) A high-power RF test setup, operational within 18 months, to enable the RF acceleration structure to be tested at liquid nitrogen temperature within a 5.5 T solenoidal field.
- (ii) A low energy muon beam test facility, operational mid-2001 to enable shakedown and calibration of the instrumentation prior to installation of the first (alternating solenoid transverse cooling) test setup late 2001, with beam measurements starting early 2002.

6.3 Funding

We have made a preliminary estimate of the cost of the R&D program based on extrapolations from (i) estimates of the cost of each component required for the cooling channel RF cavities, (ii) a general study of solenoid cost as a function of stored energy made by M. Green, and (iii) the existing Fermilab-BINP contract for lithium lens development. The required funding is summarized in Table 13. The preliminary estimate of the cost of the six-year program is \$37 M. This does not include the cost of constructing the muon beamline, installing utilities or other costs associated with preparation of the facility, or installation of the cooling apparatus, and no contingency has been included in our estimates. Table 14 summarizes the estimated funding profile needed to accomplish the schedule shown in Fig. 38. We note that the calendar year 1998 projects shown in

Task	YEAR						
	1998	1999	2000	2001	2002	2003	2004
RF Development 3 cell cavity development High power test	█	█	█				
Alt. Sol. 2m Section 1st module development 1st module bench test Solenoid Design Solenoid Fabrication LH2 design + fabrication Assembly + Bench Test Installation Beam Test		█	█	█	█		
Alt. Sol. 10m Channel RF module production Klystrons, power supplies Solenoid production L H2 production Assembly + Bench Test Installation Beam test			█	█	█	█	█
Wedge Channel Design Fabrication Beam test			█	█	█	█	
Lithium Lens Channel First 1m lens design First lens fabrication First lens bench test Second lens design 2nd lens + PS fabrication Second lens bench test Lens Beam test	█	█	█	█	█	█	█
Wedge/Lens Hybrid Design Fabrication + Bench Test Beam Test				█	█	█	█
Cooling Test Facility Prototype instrumentn Bent solenoid design Bent solenoid fabrictn Cavity fabrication Construct instrumentn Installation Shakedown	█	█	█	█	█		

Figure 38: Provisional overall R&D plan.

Table 13: Summary of estimated costs. Contingency is not included.

Item	Cost (\$)	Subtotals (\$)
Low Level Cavity Development		260,096
Material properties testing	67,000	
FNAL Be windows	61,328	
LBL low level cavity	104,256	
LBL cryogenics system	27,512	
High Power Cavity Tests		1,115,900
FNAL Be windows	61,328	
LBL high power test cavity	105,333	
LBL SC solenoid	485,000	
FNAL vacuum system	56,749	
FNAL cryogenic high power	96,098	
FNAL klystron modulator	286,392	
FNAL low level RF	25,000	
Alternating Solenoid Channel		16,000,000
SC Solenoids	9,300,000	
Accelerating cavities	900,000	
RF power	5,000,000	
Liquid hydrogen	800,000	
Lithium Lens Development		4,900,000
1m Li lens development	1,600,000	
2nd Li lens development	2,300,000	
Wedge/lens development	1,000,000	
Cooling Wedge Development		5,400,000
Design	200,000	
Purchase + Fabricate	4,000,000	
Bench test	200,000	
Test in beam	1,000,000	
Cooling Instrumentation		9,400,000
Design + prototype	400,000	
Solenoids	2,000,000	
Time cavities	1,000,000	
Detectors	5,000,000	
Bench test	500,000	
Test in beam	500,000	
Total	37,075,996	

Table 14: Estimated funding profile. Contingency is not included.

Calendar Year	Funds (M\$)
1998	0.7
1999	4.2
2000	8.5
2001	12.0
2002	9.8
2003	1.8
Total	37.0

our R&D plan are already partially funded by using part (\$570 K) of the muon collider support recieved from the DOE for this FY.

7 Summary

We propose to conduct a six-year R&D program to develop the hardware needed for ionization cooling, and demonstrate the feasibility of using the ionization cooling technique to produce cooled beams of muons for a muon collider. Our goal is to develop the cooling hardware to the point where a complete cooling channel can be confidently designed for the First Muon Collider. To accomplish this, vigorous R&D efforts are required to develop an appropriate cooling channel RF structure, design, construct, and test a section of an alternating solenoid transverse cooling channel, design, construct, and test a wedge cooling section, and develop long liquid lithium lenses. To study the performance of these cooling elements in a low energy muon beam we will require an ionization cooling test facility, consisting of a low energy muon beam, instrumentation to precisely measure the muons upstream and downstream of the cooling hardware, and an experimental hall sufficiently large to accomodate the cooling setup. We estimate the cost of this R&D program to be \$37 M (preliminary) plus the costs associated with preparing the test facility and installing the cooling apparatus. We have not included contingency in this estimate.

References

- [1] A. Sessler R. B. Palmer, A. Tollestrup, in *Proceedings of the 1996 DPF/DPB Summer Study on High-Energy Physics Snowmass'96*, New Directions for High-Energy Physics (Stanford Linear Accelerator Center, Menlo Park, CA, 1997).

- [2] Muon Collider Collaboration, in *Proceedings of the 1996 DPF/DPB Summer Study on High-Energy Physics Snowmass'96*, New Directions for High-Energy Physics (Stanford Linear Accelerator Center, Menlo Park, CA, 1997), for updated information, see the Muon Collider Collaboration WEB page at the URL, <http://www.cap.bnl.gov/mumu/>. See Ref. [1].
- [3] The Muon Collider Collaboration, Status Report of a High Luminosity Muon Collider and Future Research and Development Plans, 1998, in preparation.
- [4] Initial speculations on ionization cooling have been variously attributed to G. O'Neill and/or G. Budker see D. Neuffer in [11].
- [5] G. I. Budker, Accelerators and Colliding Beams, Proc. of the 7th International Acc. Conference (Erevan), 1969.
- [6] G. I. Budker, International High Energy Conference (Kiev), 1970.
- [7] V. V. Parkhomchuk and A. N. Skrinsky, Ionization Cooling: Physics and Applications, Proc. 12th Int. Conf. on High Energy Accelerators, 1983, eds. F. T. Cole and R. Donaldson.
- [8] A. N. Skrinsky and V. V. Parkhomchuk, Sov. J. of Nucl. Physics **12**, 223 (1981).
- [9] D. B. Cline, in *Proceedings of the Physics Potential & Development of $\mu^+\mu^-$ Colliders. 2nd Workshop*, edited by D. B. Cline (AIP Press, Woodbury, New York, 1995), Vol. 352, p. 3.
- [10] D. Neuffer, "Colliding Muon Beams at 90 GeV", FNAL Report -FN-319, 1979.
- [11] D. Neuffer, Part. Acc. **14**, 75 (1983).
- [12] D. Neuffer, in *Advanced Accelerator Concepts* (AIP Press, Woodbury, New York, 1987), Vol. 156, p. 201, see also [7, 10, 33].
- [13] R. C. Fernow and J. C. Gallardo, Phys. Rev **E52**, 1039 (1995).
- [14] U. Fano, Ann. Rev. Nucl. Sci. **13**, 1, 1963.
- [15] *High Energy Particles* (Prentice-Hall, Inc., Englewood Cliffs, NJ, 1952).

- [16] R. B. Palmer (unpublished).
- [17] A. Van Ginneken, Nucl. Instr. Meth **A 362**, (1995).
- [18] J. Bahr et al., "High Precision Particle Tracking with a Fiber Detector at the HERA ep-Collider," *SCIFI 93 Workshop on Scintillating Fiber Detectors*, Notre Dame, IN (1993) p. 183.
- [19] R. Fernow, fortran program to simulate muon ionization cooling (unpublished).
- [20] H. Kirk, Parmela modeling of alternating solenoids, presented at the Mini-Workshop on Cooling BNL, unpublished., 1998.
- [21] P. LeBrun, Alternate solenoid in DPGeant, presented at the Mini-Workshop on Cooling, BNL, 1998.
- [22] D. Neuffer and A. Van Ginneken, presented at the Mini-Workshop on Cooling, BNL Jan. 1998 (unpublished).
- [23] G. Silvestrov, Proceedings of the Muon Collider Workshop, February 22, 1993, Los Alamos National Laboratory Report LA-UR-93-866 (1993).
- [24] B. Bayanov et al., Nucl. Inst. and Meth. **190**, (1981).
- [25] C. D. Johnson, Hyperfine Interactions **44**, 21 (1988).
- [26] M. D. Church and J. P. Marriner, Annu. Rev. Nucl. Sci. **43**, 253 (1993).
- [27] G. Silvestrov, in *Proceedings of the 9th Advanced ICFA Beam Dynamics Workshop*, edited by J. C. Gallardo (AIP Press, Woodbury, New York, 1996), Vol. 372.
- [28] The 200 kJ pulser and power converter for the 36 mm lithium lens of the antiproton accumulator and collector (AAC) at CERN, CERN report CERN PS 89-61 PO, 1989.
- [29] K. T. McDonald C. Lu and E. J. Prebys, A Detector Scenario for the Muon Cooling Experiment, Princeton/ $\mu\mu$ /97-8; see also <http://www.hep.princeton.edu/>, 1997.
- [30] Technical Data Sheet. Fine Mesh PMT Series for High Magnetic Field Environments.

- [31] V. Sum et al., Nucl. Instr. and Meth. **A326**, 489 (1993).
- [32] H. Kichimi et al., Nucl. Instr. and Meth. **A325**, 451 (1993).
- [33] in *Proceedings of the Mini-Workshop on $\mu^+\mu^-$ Colliders: Particle Physics and Design*, edited by Nucl. Instr. and Meth. (North-Holland, The Netherland, 1994), Vol. A350.